Data in brief: Energy performance evaluation of alternative energy vectors for subsonic intercontinental tube-wing aircraft

Swapnil S. Jagtap [a*], Peter R.N. Childs [b] and Marc E.J. Stettler [a]

[a] Centre for Transport Studies, Department of Civil and Environmental Engineering, Imperial College London, London SW7 2AZ, United Kingdom

[b] Energy Futures Lab, Imperial College London, London SW7 2AZ, United Kingdom

* Corresponding author: swapniljagtap111@gmail.com

Abstract:

This is additional data to the main paper publication

Link to the main paper:

https://www.sciencedirect.com/science/article/abs/pii/S136192092200414X

Nomenclature

ASTM	American Society for Testing and Materials	LTA	Large twin aisle
ATJ	Alcohol-to-jet	L/D	Lift to drag ratio
C_D	Total drag coefficient	MTOW	Maximum take-off weight
C_f	Skin friction coefficient	NO_x	Oxides of nitrogen
C_L	Lift coefficient	OEW	Operating empty weight
CO	Carbon monoxide	PtL	Power-to-liquid fuel
CO_2	Carbon dioxide	R	Range
d_f	Fuselage diameter	SEC	Specific energy consumption
FCS	Fuel cell systems	SO_x	Oxides of sulphur
FCH	Fuel Cells and Hydrogen	SPK	Synthetic paraffin kerosene
FR	Fineness ratio	STJ	sugar-to-jet fuel
FT	Fischer–Tropsch	S_{wet}	Aircraft wetted area
g	Acceleration due to gravity	$S_{wet,\ Fuselage}$	Fuselage wetted area
GHG	Greenhouse gas	TeDP	Turbo-electric distributed propulsion
		VLTA	Very large twin aisle
GTOW	Gross take-off weight	$W_{aircraft}$	Aircraft weight in cruise
h	Lower calorific value	$W_{initial}$	Initial cruise aircraft weight
HEFA	Hydro-processed esters and fatty acids	W_{final}	End of cruise aircraft weight
HRJ	Hydro-processed renewable jet fuel	$W_{Fuselage}$	Aircraft fuselage weight
IATA	International Air Transport Association	$W_{F,block}$	Block fuel weight
LCV	lower calorific value	W_p	Passenger payload weight
l_f	Fuselage length	ΔL	Additional fuselage length for alternative liquid fuels
LH_2	Liquid hydrogen	η	Gravimetric index
LNG	Liquid natural gas	η_o	Overall efficiency
LNH_3	Liquid ammonia		

SI 1. Detailed literature review of aircraft propulsion technologies, energy vectors and alternative fuels

SI 1.1 Alternative liquid fuels

The exhaust of an aircraft operating on conventional jet fuel includes carbon dioxide (CO_2), water vapour, nitrogen oxides (NO_x), carbon monoxide (CO), unburned hydrocarbons, sulphur oxides (SO_x), traces of hydroxyl family and nitrogen compounds, soot, volatile organic compounds, organic carbon, particulate matter, and normal atmospheric oxygen and nitrogen [1].

Liquid fuels such as synthetic jet fuel, hydrogen (liquid hydrogen, natural gas, ammonia), ethanol and methanol are explored in literature as alternative aviation fuels [2], [3]. Amongst these, the synthetic fuel like biomass derived jet fuel has been extensively explored in technical literature. Performance characteristics of an aircraft powered by natural gas, ammonia, ethanol, and methanol, especially for intercontinental travel are less published.

1.1.1 Synthetic jet fuels

Synthetic jet fuels are fuels manufactured from non-crude oil feedstocks/pathways but have (almost) similar operational performance as that of conventional jet fuel (Jet-A). Non-crude oil feedstocks/pathways include other fossil fuels, biomass, and power-to-liquid pathway. These fuels, especially bio-jet fuel pathways, are interesting particularly because of their potential to significantly reduce the life-cycle GHG emission from the aviation sector, depending on the feedstock type/source [4]. However, the current work focusses on the use phase of the aircraft. Therefore, the literature review does not include life cycle-based studies or metrics of synthetic jet fuels.

Not all bio-jet fuels (i.e. fuel from different production pathways) can be directly used in current aircraft (known as drop-in fuels), because some of fuel properties and chemical

contents are not same as that of the conventional jet fuel [5]. Drop-in fuels are the fuels that can be directly used in the present aircraft without any modifications. Some systems within the aircraft are designed considering the properties of conventional jet fuel. For example: The aromatic content of conventional jet fuel causes rubber seals used in the high-pressure fuel system to swell, thereby preventing fuel leakage during aircraft operation at different altitudes; and synthetic paraffin kerosene (SPK) jet fuel cannot be used in neat form (100%) without modifications to the present aircraft or without the addition of synthetic aromatics/additives [5]. The difference in fuel properties of 100% SPK and Jet-A fuel, and related operability issues are detailed in resources [5], [6]. American Society for Testing and Materials (ASTM) has approved four bio-jet fuel pathways which can be used in aircraft as drop-in fuels [6]–[10]. These are:

1. Fischer-Tropsch (FT) SPK (FT-SPK) with maximum 50% blend and syngas FT with aromatic alkylation (FT-SPK/A) with maximum 50% blend.
2. Hydro-processed lipids/hydro-processed renewable jet fuel or hydro-processed esters and fatty acids (HRJ/HEFA-SPK) with maximum 50% blend,
3. Bio-chem sugars or hydro-processed fermented sugars to synthetic iso-paraffins (HFS-SIP) with maximum 10% blend (also referred to as sugar-to-jet (STJ) fuel), and
4. Alcohol-to-jet (ATJ-SPK) fuel with maximum 50% blend (recently revised from 30% blend),

where the blending is done with the conventional jet fuel.

A study by Blakey et al. [11] reveals that the use of FT-SPK can help in reducing the local air-quality as a result of reduced particulate matter release. Also, the use of correct alternative fuel has the potential to make aviation sector carbon neutral. Study by Hileman et al. [12] examines performance of bio-jet fuels based on a first-order approach using the Breguet range equation. The results from this study show that the fleet-wide (hypothetical) use of pure

(100%) SPK (not approved currently) can decrease aircraft energy consumption (in-flight) by 0.3%. The (separate) use of 10% blended SPK (STJ) and 50% blended SPK (ATJ, HEFA or FT) can reduce the aircraft energy consumption (in-flight) by 0.03% and 0.15% respectively [9], [10], [13]. Test flights using biofuels (SPK) from algae and camelina were successfully conducted which marks the beginning of using alternative fuel in aviation [5], [6], [14]. Additionally, Lufthansa successfully completed a six-month flight-operation using 50% blended biofuel on Airbus A321 between Hamburg and Frankfurt, without any technical problems or operational inconsistencies [5], [6], [15]. In recent years many test flights have been conducted on regional jet (ATR aircraft) [16], business jets [17], and LTA (A350) and VLTA (A380) [18], powered by 100% SPK primarily from HEFA pathway using waste biomass. From these test flights, no major issues were reported.

A study by Schmidt et al. [19] demonstrates the development of a relatively novel fuel called power-to-liquid (PtL) jet fuel. Electricity produced from renewable sources like solar and wind energy is used in the electrolysis of water for hydrogen production. After carbon (CO_2) capture, hydrogen and CO_2 undergo chemical process to form hydrocarbon fuel (PtL). This study provides information on different scenarios of producing PtL fuel, and it estimates the life-cycle greenhouse gas (GHG) from the production pathways. PtL fuel produced from renewable energy has significantly lesser/near-zero lifecycle GHG emission compared to conventional jet fuel. It is not currently approved for civil aviation. Its thermo-physical and fuel handling properties are like conventional jet fuel, which means that PtL can be potentially used as a drop-in fuel. This enables status-quo in aircraft powerplants. One of the process involved in fuel refining is FT process. It is to be noted that 50% blended FT jet fuel is approved by ASTM, and 50% blend of PtL from FT process can be used directly.

1.1.2 Hydrogen

Hydrogen is the most abundant element in the universe. It is a suitable energy storage medium which is carbon free and does not include other impurities. Hydrogen can be stored as: a pressurized gas, a hydride, liquid hydrogen, or slush or solid form. Examples of hydride include methane, ammonia, etc. Storage as slush or solid hydrogen demands high energy to sub-cool the fuel and its use only leads to nominal savings in fuel tank volume and weight [20]. Hydrogen storage as a super-saturated (subcooled) liquid can cause high pressure fluctuations inside the tank thereby resulting in heavier tanks. Hydride and gaseous storage are impractical because of the excessive tank weight or volume resulting from carrying a fuel of low energy density per unit volume especially for gaseous hydrogen [20], [21]. However, it is to be noted that methane combustion produces carbon emissions, and ammonia combustion cannot be called a self-sustained combustion process (poor flammability characteristics) and it produces higher NO_x [22]–[24].

Liquid hydrogen (LH_2) as an aviation fuel comes across as an interesting candidate, primarily because of its higher energy density (lower calorific value [LCV]) of 120 MJ/kg compared to conventional jet fuel's LCV of 43.2 MJ/kg [25], and because hydrogen combustion does not release emissions like CO_2, CO, volatile organic compounds, particulate matter ($PM_{2.5}$ and PM_{10}), black and organic carbon, and SO_x, during direct-use. The high energy density (LCV) of LH_2 for aviation application can be utilised via fuel cells and gas turbine engines (hydrogen combustion). Fuel cell powered aircraft would only emit water vapour. For a gas turbine engine powered aircraft (hydrogen combustion), the products of combustion include water vapour and NO_x. Khandelwal et al. [26] review different LH_2 tank and insulation configurations, hydrogen engines, ultra-low NO_x combustors and safety aspect. Additionally, Rondinelli et al. [27] discuss the airport systems design and operation associated with the transition from Jet-A fuel to LH_2 fuel.

LH_2 is a special fuel because it is 2.78 times more energy dense per mass than conventional Jet-A fuel but the conventional Jet-A fuel is 4.1 times more energy-dense per volume compared to LH_2 [2]. This implies that the fuel tanks on LH_2 powered aircraft will require more volume storage (bigger tanks with insulation), which will further increase aircraft weight. The cryogenic LH_2 tanks would be installed in the fuselage. To maintain the same payload capacity, it is necessary to design the aircraft (fuselage, mechanical stresses, stability, and wing-loading for a conventional tube-wing aircraft) to account for the extra fuselage and fuel tank weight.

A study by Prewitz et al. [28] simulates the performance of a regional hydrogen powered aircraft (ATR-72) that has a design range of 1,324 km (715 nautical miles) for maximum payload of 7,050 kg. This study estimates the critical value of the cryogenic tank gravimetric index of 0.33 – 0.35 that could enable economic flight operations, while that required to meet the design target range is 0.19 (present technology already supports the required value). A study by Yang et al. [29] models a small single aisle LH_2 aircraft (range 5,480 km with 177 passengers) and examines the environmental impact of a fleet of this LH_2 aircraft on a world-wide network. The authors use the Fleet-Level Environmental Evaluation Tool (FLEET) tool to model different scenarios and estimate equivalent carbon emissions and LH_2 cost. The study finds that that by introducing a (small) single aisle LH_2 aircraft (in 2035) could reduce fleet-level carbon emission by 9.96% in comparison with a baseline with no liquid hydrogen aircraft. A thesis by Svensson [30] simulates a medium range LH_2 aircraft that seats 185 passengers over a range of 7,400 km. The design of this aircraft is carried out in a design environment called PIANO (and also referencing to the Cryoplane study [31]). The energy consumption of this LH_2 aircraft increases by 10% compared to a reference Jet-A aircraft. A study by Silberhorn et al. [32] designs LH_2 aircraft seating 165 passengers with range of 5,740 km. The authors design three LH_2 aircraft, each having a distinct cryogenic tank installation

configuration – aft of fuselage, on top of fuselage (best energy performance), and wing podded. Depending on the type of tank installation, the energy consumption of the LH_2 aircraft increases by 6.5 – 7.5% compared to the baseline Jet-A aircraft. Above studies on combustion based LH_2 aircraft [28]–[30], [32] model the energy performance of a regional/small- to mid-size aircraft for a short- to medium-range application only.

A study by Cipolla et al. [33] designs LH_2 powered small– and medium–range aircraft, where a box-wing aircraft concept is a reference aircraft that has 5,722 km range seating 308 passengers. The authors primarily consider two fuselage/cabin layouts (for installing LH_2 tanks) that affect the passenger seating and range. For one of the layouts the passenger seating is 308 but the range (<=4,000) reduces. However, for the other layouts the passenger seating is between 164 and 196, and their corresponding ranges are 6,000 km and 4,000 km, respectively. A study by Gomez et al. [34] models the performance of an LH_2 powered tube-wing aircraft. The reference aircraft seats 296 passengers with range of 6,500 km. The modified version of this aircraft for LH_2 use seats 194 passengers with range of 9,000 km, and the fuselage length is equal to the reference aircraft. For this LH_2 powered tube-wing aircraft, the cryogenic tank η is 0.826 for the rear tank and 0.741 for the forward tank. The authors conduct a detail structural and stress analysis of the cryogenic tanks, where the tanks are of integral type made of Aluminium alloy employing polyurethane insultation. Above studies [33], [34] designed LH_2 aircraft for different (smaller) payload and range combination compared to the reference long-range LTA aircraft.

A study by Troeltsch et al. [35] design an LH_2 aircraft (range 11,853 km with 400 passengers) with foam-based LH_2 tanks (front and aft). In contrast to other studies on LH_2 aircraft design the authors choose to reduce the cruise Mach speed from 0.82 of the reference Jet-A aircraft to 0.7, and this LH_2 aircraft shows a 9% increase in energy consumption compared to the reference aircraft. A study by Proesmans et al. [36] conducts a pareto-optimal

design examination of LH_2 and 100% SPK (separately) powered aircraft for short, medium and long range aircraft, where each fuel and aircraft type is designed separately for minimising climate impact and cash operating costs. The result of this approach is that for a given aircraft type and optimisation objective, each aircraft fuelled by respective fuel may vary from the baseline in terms of wing loading, aspect ratio, engine BPR, pressure ratio of fan and compressors, turbine inlet temperatures, and most importantly cruise Mach, and cruise altitude. Therefore, for a given aircraft type and optimisation objective, a very few aircraft design and performance features are similar to the baseline. For climate impact minimisation optimisation objective, it is observed that the cruise altitude and cruise Mach are similar for Jet-A, LH_2, and 100% SPK. The energy performance of Jet-A and 100% SPK is same. LH_2 fuel shows 7.6% decrease in MTOW, 22.8% increase in OEW, 41.1% increase in fuselage length, and 12.9% increase in energy consumption. Above studies [35], [36] design LH_2 aircraft, where the cruises at lower Mach and/or altitude and has different aircraft design characteristics compared to the typical baseline long-range LTA aircraft.

A study by Grewe et al. [37] examines the climate impact of a futuristic multi-fuel BWB aircraft seating 300 passengers for design range of 14,000 km. For this aircraft 33% of energy is provided by bio-kerosene and 67% energy either comes from LNG or LH_2. It is to be noted that this aircraft design performance is based on an extremely simple model as it does not take into account details such as the cryogenic storage requirements and the associated drag and weight penalty. The study finds that LNG – bio-kerosene has lower climate impacts compared to LH_2 – bio-kerosene and the conventional aircraft. This study does not model an aircraft completely powered by LH_2 fuel.

1.1.3 Comparative study between different alternative liquid fuels

Alcohols such as methanol and ethanol are alternative liquid fuels that are less explored in literature. Additionally, there is just one study which compares performance of different

alternative liquid fuel, that too for a small aircraft medium-range application. Bicer et al. [2] conducts a first order evaluation of a small twin aisle aircraft of conventional tube-wing architecture (such as the Boeing 767) with a flight range of 5600 km, where the aircraft is operated by Jet-A, LH_2, liquid natural gas (LNG), liquid ammonia (LNH_3), ethanol and methanol. It is to be noted that the authors use SimaPro software, which is a life-cycle assessment software for their analysis. Bicer et al. find that the energy consumption of an aircraft powered by LH_2, LNG, LNH_3, ethanol and methanol are 8.62, 12.53, 9.53, 9.8 and 9.8 MJ/tonne-km respectively compared to energy consumption of 9.35 MJ/tonne-km for conventional jet fuel. The methodology used by the authors for estimating the energy consumption of the aircraft (use-phase) is not clear from the information provided in the said publication. It appears that the said study evaluates aircraft performance purely based on the gravimetric energy densities of different fuels. The low volumetric energy density of these alternative fuels especially cryogenic fuels such as LH_2, LNG, LNH_3 compared to Jet-A, have significant aircraft design (weight and drag) implications which affect the performance.

1.1.4 Studies providing a future roadmap for the use of alternative liquid fuel

A study by Daggett et al. [3] provides fuel solutions for the future to reduce the environmental impact of aviation. Daggett et al. propose 50/50 blend of FT-SPK/conventional jet fuel to be used in present day aero engines as a near-term solution; 0-50% HEFA-SPK (hydro-processed esters and fatty acids) with 100-50% FT-SPK to be used in advanced engines like inter-cooled recuperated engines, and ultra-high bypass ratio engines like geared turbofan engines and un-ducted propfan as a mid-term solution; and LH_2 and/or LNG to be used in cryo-fuelled engine as a long-term solution to dramatically reduce aviation sector's GHG emissions.

Rolls Royce [38] evaluates a range of alternative fuels and propulsion technology towards making aviation more sustainable. The alternative fuels comprise of:

a. SPK produced from non-crude oil sources but fossil-fuel sources (typically using FT process),
b. Biomass derived SPKs (using FT, ATJ, STJ and HEFA manufacturing pathways), and
c. Fuel produced from renewable electricity.

In the first kind of alternative fuel, hydrotreated pyrolysis oil (from fossil fuel), coal (coal to liquid), natural gas, and/or flue gas (gas to liquid) are used for producing SPKs typically using FT synthesis [10]. Biofuels (second type of alternative fuel) produced from crops that compete with food are termed as first-generation biofuels, while those produced from non-food crops that require arable land for cultivation are termed as second generation or advanced biofuels. Biofuel produced from algae: a non-food 'aquatic' crop, is termed as third generation biofuel. The third type of alternative fuels comprise of fuels produced from electrochemical synthesis, where the manufacturing process uses electricity produced from renewable sources. Broadly, the third type of alternative fuels can be categorized into carbon-rich and carbon-lean fuels. PtL fuel is a carbon rich fuel, as it is essentially an SPK which is chemically similar to the conventional jet fuel (Jet A) [39]. Fuels which are rich in hydrogen content fall under the category of carbon-lean fuels. According to Rolls Royce [38], drop-in SPKs (like biofuels, FT fuel, PtL fuel) and LH_2 fuel could be used in future for medium to long range aircraft applications.

A recent report by World Economic Forum [40] based on Aviation Impact Accelerator program provides insights into pathways that could make aviation climate neutral. This study explores for alternatives to Jet-A other than SPK. This study finds that for short-range, battery–electric aircraft utilising renewable electricity could be less carbon intense than conventional aircraft (<400 km in 2035, <600 km in 2050). This study points out the need to improve battery life cycles and management, and advance battery-electric aircraft energy density. For medium-range flight, fuel cell (LH_2) powered aircraft could provide a low-carbon alternative to Jet-A

powered aircraft (<2000 km in 2035 and <4000 km in 2050). This study emphasizes the need to develop lighter fuel cell systems. Lastly, for long-range travel combustion based LH_2 aircraft could cause lesser climate impacts than Jet-A fuel. Overall, for LH_2 as a fuel (fuel cell based and combustion based), this study points out the need to: accelerate the introduction of green hydrogen, develop low weight cryogenic tanks, and redesign aircraft (not retrofit) for optimised hydrogen performance. Additionally, this study emphasises the need for more detailed research that would improve confidence levels of prediction of climate effect of contrails and mitigation strategies, especially for LH_2 fuel.

1.1.5 Summary of literature review on alternative liquid fuels

Different approved blends of drop-in SPKs are currently the alternative to Jet-A fuel. Based on the literature review, methanol, ethanol, 100% SPK and hydrogen (LH_2, LNG and LNH_3) appear to be future alternatives to the conventional Jet-A fuel based on their properties. The feasible form of hydrogen uses i.e. LH_2, LNG or LNH_3 needs further (quantitative) examination. The methodology used by Bicer et al. [2] for estimating the energy consumption of the aircraft (use-phase) is not clear and it appears that they evaluate the aircraft performance purely based on the gravimetric energy densities of different fuels. The low volumetric energy density of these alternative fuels especially cryogenic fuels such as LH_2, LNG, LNH_3 compared to Jet-A, have significant aircraft design (weight and drag) implications which affect the performance. Therefore, a more detailed analysis is required which quantitatively evaluates the six fuels – methanol, ethanol, 100% SPK, LH_2, LNG and LNH_3. There are technological challenges associated with the use of these fuels in the present aircraft type as modifications are required. However, in the next (future) generation of aircraft fleet that will have technological improvements, the required modifications could be done to the aircraft in the design stage itself for the use of the respective alternative liquid fuel.

SI 1.2 Solar-electric and ion propulsion

Solar impulse [41], is the world's first solar-powered aircraft with a seating capacity of one passenger and it has successfully toured the globe. This propulsion technology requires significant improvement for enabling a commercial long-range flight of ~300 passengers.

An ion-based propulsion method has been applied to a model aircraft (no passengers) by researchers at MIT, and test flights have been conducted [42], [43]. This flight starts with a (manual) ramped slingshot take-off and the ion-propulsion is used during steady level flight. There needs to be a dramatic improvement in this technology for enabling typical long-range Mach 0.85 flight of ~300 passengers along with safety considerations.

SI 1.3 Batteries and turbo-electric

A study by Grönstedt et al. [44] finds that aircraft fuel is currently 50-100 times more power dense than batteries and historical improvement rate of 2-3% makes it uncertain whether batteries will reach the power density required for (approximately) year 2050 timeframe. Brelje et al. [45] raise safety concerns, as batteries are a known aviation hazard and have much less service experience and fail in seemingly more-complex modes. The design of economically viable fixed-wing electric-aircraft demands high-end technology. Figure SI 1 provides the specific energy of different battery technologies as compared with the energy density of kerosene/conventional jet fuel (Jet-A). It is to be noted that Figure SI 1 is on a log-scale, and there is an order of magnitude difference between the specific energy of the best state-of-the-art battery technology and conventional jet fuel.

The current battery energy density is 100-265 Wh/kg [46], [47]. Pornet et al. [48] investigated the use of batteries as energy source alongside conventional jet fuel, as a retrofit for short-to-medium range single-aisle turbofan aircraft. They conclude that the use of batteries with an energy density of 1500 Wh/kg, as an energy source, can provide a block fuel reduction

(of 16%) on short-range missions. Further analysis by Pornet et al. demonstrates that batteries with an energy density below 1000 Wh/kg provide no significant fuel savings at all. Voskuijl et al. [49] examine the use of 1000 Wh/kg energy density batteries for powering a 70 passenger regional turbo-prop aircraft with a range of 1528 km, comprising of 34% electric shaft power. The authors do not account for the turbo-prop noise effects in this study. This arrangement results in 28% reduction in mission fuel, but it comes at the expense of a larger aircraft in terms of weight and wing area. In a study by Friedrich et al. [50], a Boeing 737–800 aircraft was retrofitted with a hybrid-electric propulsion system. Assuming a specific energy of 750 Wh/kg, 10.4% fuel saving was computed on a two-hour mission. According to studies by Pornet et al. and Voskuijl et al., the current technology is not ready, and significant development in battery technology is required for hybrid-electric aircraft, especially for a long-range 300 passenger aircraft.

The study by Schäfer et al. [51] uses battery packs of 800 Wh/kg for an aircraft completely powered by batteries. This full-electric aircraft seats 150 passengers for a range of up to 1,111 km. The authors find that this full-electric aircraft could replace half of all aircraft departures and has the potential to decrease fuel use and direct CO_2 emissions by 15%. Additionally, this full-electric aircraft can decrease the airport NO_x emissions by 40%.

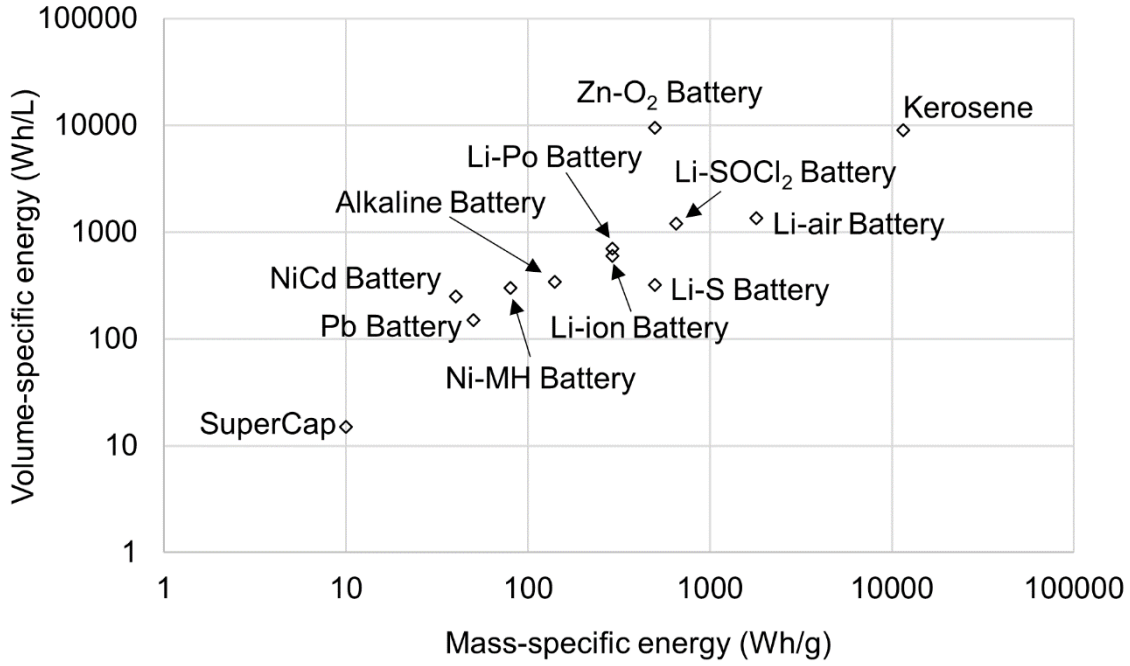

Figure SI 1. Specific energy of different battery technologies as compared to the energy density of kerosene/conventional jet fuel (data source [47]**)**

The study by Ashcraft et al. [52] reviews several hybrid-electric aircraft concepts that use multiple futuristic technologies such as batteries, fuel cells and boundary layer ingestion. This study includes feasibility criteria and constraints for such futuristic aircraft concepts. These hybrid-electric aircraft concepts are further analysed and compared in detail with systems engineering approach, and it is found that NASA N3-X turbo-electric distributed propulsion (TeDP) is the best concept that can meet NASA's rigorous design goals in 2035 timeframe [53]. The NASA N3-X turbo-electric distributed propulsion (TeDP) is expected to offer dramatic energy consumption reduction [52]. The electric motors and boundary layer ingestion (BLI) require significant technological developments. The BLI affects the propulsion system design due to flow distortion, and it has to be accurately included within the propulsion system design and optimization via high-fidelity multi-physics approach [54]. As per Ashcraft et al. [52], fuel cells are unlikely to be ready for powering propulsion systems on large aircraft

by year 2035 but they are more likely to be used for augmenting a primary power source. Additionally, considering past battery development cycles it is unlikely that new chemistries will be available for year 2035 advanced concepts. NASA N3-X TeDP concept uses novel propulsion system, which utilizes superconducting electrically driven, distributed low-pressure-ratio fans with power provided by two remote superconducting electric generators [55]. The turbo-generators are located at the wing tips, while the fans are positioned at the rear of the planform where they ingest the boundary layer. NASA N3-X TeDP concept has the potential to reduce fuel consumption by 70-72%. For this concept it is assumed that the required power density of the generators and motors is achieved from wound rotor synchronous machines with superconductor windings on stator and rotor. For keeping the required cooling capacity within acceptable limits, the stator conductors must be engineered carefully for reducing the AC losses. The required filament size for enabling this presently appears achievable only for the superconductor MgB_2. The critical temperature (the highest temperature at which it is superconducting) for MgB_2 is only 39K, and it must be below 30K for producing useful current density. Although Bismuth Strontium Calcium Copper Oxide cannot be manufactured presently with acceptable AC losses, a future development is assumed which makes it possible. Motors and generators with a hypothetical fine-wire Bismuth Strontium Calcium Copper Oxide are assumed. Additionally, according to Ashcraft et al. [52], superconducting electric motors are extremely important to the success of NASA's N3-X TeDP concept. The limitations of using the said superconducting system is the increased system complexity. Along with the electric motors, other components such as a compressor, cryocooling system, inverter, and power source would also need to be added. The viability is closely related to the development of boundary layer ingestion and superconducting electric motor/generators that will eliminate mechanical connections for power distribution.

Researchers at the University of Cambridge have developed a single-seater hybrid-electric aircraft (battery energy density not known) and have flown it successfully [56]. For the 2040 timeframe, DLR researchers are developing a 70 seater hybrid-electric aircraft (battery energy density unknown) with a range of 2,000 km [57]. According to Rolls Royce [38], all-electric propulsion can power a small aircraft with short range. This is typically a regional and single-aisle aircraft category. Moreover, hybrid-electric aircraft technology can be used for typical medium range aircraft, and potentially with its range extended to slightly higher range.

Overall, the assumption of battery energy density reaching 4-8 times the present capacity, the maximum fuel consumption reduction of 28% is observed in a short-range turbo-prop aircraft seating 70 passengers. Additionally, if life-cycle effects are taken into consideration, the savings in fuel consumption come at the expense of extra electricity production or emissions elsewhere which is also sensitive to the energy-mix of a country/region (thermal vs renewable power production). Battery powered aircraft (hybrid or full electric) appear to be technologically infeasible for large long-range aircraft. However, this is a fast-moving area subject to step-changes in technology in terms of battery performance and associated systems as demonstrated for example in the recent Spirit of Innovation aircraft [58]. Studies by Mukhopadhaya et al. [59] and FlyZero report [60] find that battery powered aircraft (hybrid and/or full electric) appear to be infeasible currently (considering future technology development trend) for enabling typical long-range flight of an LTA aircraft.

A study by Dietl et al. [61] designs a turbo-electric aircraft called Polaris which is powered by LH_2 fuel (stored in foam based tanks) employing N+3 technology and an unconventional aircraft architecture with open rotor engines. This aircraft seats 150 passengers with 2780 km at design point. A study by Druot et al. [62] model turbo-electric aircraft fleet powered by LH_2 fuel by employing different configurations of fuel tank integration. The study

finds that such a propulsion technology enables range and payload combination only for a single aisle type of aircraft with short-range application.

Overall, electric aircraft (turbo and/or battery electric – hybrid and/or full electric) appear to be infeasible currently and require dramatic improvement for enabling typical long-range Mach 0.85 flight of an LTA aircraft.

SI 1.4 Fuel cells

In 2016, the world's first four-seater passenger aircraft (range of up to 1,500 km) powered by fuel cells and battery system called 'HY4' made its first flight [57]. According to Rolls Royce [38], small size and short range aircraft can be powered by LH_2 fuel by using proton exchange membrane (PEM) fuel cell. The aircraft range can further be extended by the use of batteries. This system of propulsion has better efficiency than small gas turbine engines and lithium-ion batteries. Additionally, for medium and long-range aircraft, direct combustion of hydrogen in gas turbine engine is the solution. However, with this system of hydrogen combustion, NO_x is produced along with water vapor, which is not the case with fuel cell as it only produces water vapour. Study by Ashcraft et al. [52] finds that fuel-cells are unlikely to be ready for completely powering propulsion systems on large aircraft by year 2035 but they are more likely to be used for augmenting a primary power source.

The fuel cell specific power metrics are typically reported for fuel cell stacks [63]. The specific power for fuel cell systems (FCS) includes important supporting and/or auxiliary components. This is based on the stack or site-specific requirements, e.g. hydrogen-, air-, water-, heat- and system-management. They are integrated into a comprehensive fuel cell system package. FCS performance is based on the functioning of non-stack systems. In terms of modelling energy systems, FCS specific power is used. In a study by Delgado Gosálvez et al. [64], a small LH_2 fuel cell powered commuter aircraft called the 'Greenliner' is designed.

The range of 'Greenliner' is 500 nautical mile (nmi) or 926 km and it seats 19 passengers. The authors have assumed a specific power capacity for the FCS similar in magnitude (2.72 kW/kg) as that of the fuel cell stacks used in the fuel cell powered car 'Toyota Mirai' (2 kW/kg). It is to be noted that the FCS specific power capacity of the fuel cell technology used in Toyota Mirai has a maximum value of 0.8 kW/kg. Additionally, the said aircraft is partially powered by lithium-sulphur battery. If the previous discussion on Rolls Royce's testing is recalled, then Rolls Royce's plan is much more ambitious (thrice the range) than 'Greenliner'. It is to be noted that this future plan despite being ambitious is limited to flight range of ~1500 nmi (~2800km), which could be representative of a fuel-cell powered single-aisle aircraft seating approximately 150 passengers.

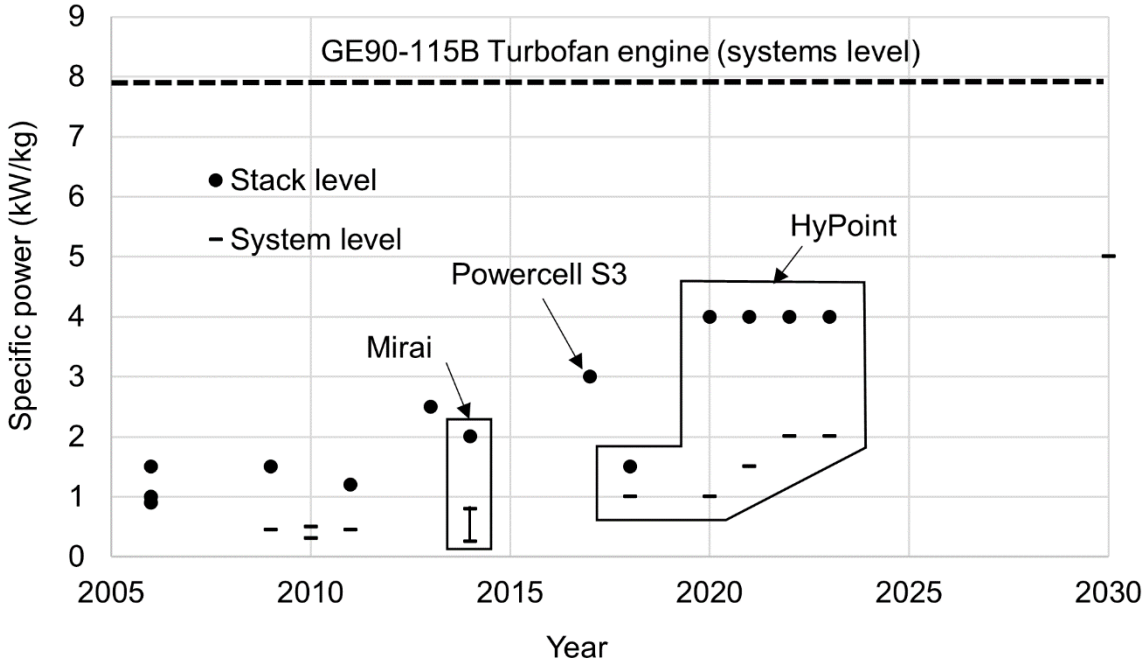

Figure SI 2. Trend of specific power of fuel cell technology and comparison with the specific power of a gas turbine engine used on Boeing 777-200LR aircraft (data source [63], [65]–[67]**)**

Figure SI 2 shows the trend of fuel cell technology development (with time until year 2030) on both stack level and systems level. On a Boeing 777-200LR aircraft (large twin aisle

or LTA), two GE90 engines are used. The fuel flow rate at take-off is known to be 4.32 kg/s from the ICAO emissions databank while using conventional jet fuel (gravimetric energy density of 43.2 MJ/kg) [68]. The overall efficiency is known to be 0.37 [69]. Additionally, the engine weight is known to be 8761 kg [70]. The specific power of this engine (systems level) is calculated to be (4.32 x 43,200 x 0.37/8761 =) 7.88 kW/kg. Therefore, from Figure SI 2 it can be concluded that fuel cells do not appear to be a technological solution for future large aircraft with a long range. In terms of hydrogen use, according to Rolls Royce's tests discussed previously, long range large aircraft need to be powered by direct combustion of LH_2 in gas turbine engines.

A study by Kasim et al. [71] models the performance of a regional aircraft (Cessna) retrofitted with fuel cell and hydrogen fuel systems. The maximum passenger seating reduces from 14 to 8, and the aircraft range is 350 km. A study by Nicolay et al. [72] examines the performance of a small/regional aircraft powered by fuel cell and hydrogen fuel systems. The maximum payload is 428 kg (or four passenger seating) with a range of 1,678 km. A study by Waddington et al. [73] models an LH_2 fuel cell powered aircraft called CHEETA of an unconventional airframe or architecture seating 180 passengers over 5436 km range (similar to a class of Boeing 737). A thesis by Vonhoff [74] designs a regional aircraft powered by fuel cell and hydrogen systems. A study by Brelje et al. [75] designs a small fuel cell powered aircraft (range ~2000 km), where the LH_2 fuel is stored in wings. The author conducts a detailed aero-structural analysis of the wings for the installation of LH_2 fuel tanks. A study by Marciello et al. [76] provide conceptual design of a fuel cell powered regional aircraft with a design range of 926 km seating 19 passengers. A study by Pastra et al. [77] models a hybrid hydrogen fuel cell and battery powered regional turboprop aircraft with a design range of 2035 km seating 74 passengers. Studies by Mukhopadhaya et al. [59] and FlyZero report [60] find that fuel cell LH_2 powered aircraft technology appear to be infeasible currently (considering future

technology development trend) and require dramatic improvement for enabling typical long-range Mach 0.85 flight of an LTA aircraft.

SI 1.5 Summary of literature review

The literature review covers studies from both academia and industry. Overall, the above review suggests that the efforts from academia and industry agree with each other and in-line with the International Air Transport Association (IATA) strategy #1 for making future aviation more sustainable.

Solar-electric and ion propulsion technology appear to be infeasible currently and require dramatic improvement for enabling typical long-range Mach 0.85 flight of ~300 passengers with passenger safety considerations. Electric aircraft (battery and turbo-electric) and fuel cell development trend could enable passenger travel only for a small short-range to medium-range aircraft. Different approved blends of drop-in SPKs are currently the alternative to Jet-A fuel. Based on the literature review, methanol, ethanol, 100% SPK, LH_2, LNG and LNH_3 appear to be future alternatives to the conventional Jet-A fuel based on their properties. As discussed in SI §1.1.5 of the present document, a more detailed analysis is required which quantitatively evaluates these six fuels.

SI 2. Overview of GasTurb 13 engine cycle design and optimization

GasTurb 13 is a software tool that estimates the performance and optimization of gas turbine engines [78]–[80]. It can perform zero-dimensional (thermodynamic cycle performance and weight estimation) and one-dimensional gas turbine analysis, which at least fall within the ambit of the conceptual engine design phase. In GasTurb 13, the details needed for professional gas turbine performance are estimated along with the engine thermodynamics. This tool also has the feature of conducting optimization of the engine thermodynamic cycle. Additionally, turbine cooling and secondary air system can be analysed with this tool. The calculations in

GasTurb are based on the engine design and performance methods and Euler turbomachinery equations [79]–[81]. The GasTurb functioning and calculation procedures are detailed in [79], [80]. Additionally, the author of GasTurb 13, simulates three different gas turbine engines i.e. J57-19W, CFM56-3 and F107-WR-400, in their book in reference [79].

SI 3. Thermodynamic cycle analysis of a turbofan engine

We conduct a simple thermodynamic analysis of a turbofan engine for constant thrust production using different fuels under consideration. This is carried out using standard set of equation for gas-turbine engines that apply Brayton cycle, which can be found in [81]–[84]. Table SI 1 lists the thermodynamic cycle analysis input and output parameters at design point. We first begin with a baseline (Jet-A) engine for producing a target thrust of 100 kN and the fuel flow rate is iterated towards this objective, for fixed input component efficiencies, ambient pressure and temperature, and air to fuel ratio.

For a given alternative fuel, the input component efficiencies, and ambient pressure and temperature remain the same as that of Jet-A, but its air to fuel ratio is calculated by multiplying the air to fuel ratio of Jet-A case with the ratio of lower calorific value of the alternative fuel and the lower calorific value of Jet-A. The lower calorific values [2], [13], and properties of combustion gas [85] for all fuel cases are known from the respective resources. For 100% SPK and ethanol, the properties of combustion gases are not known. We assume that the combustion gas properties of 100% SPK and ethanol are same as that of Jet-A and methanol, respectively. Similar to the Jet-A case, the fuel flow rate for engine powered by a given alternative fuel is iterated towards the objective of producing a target thrust of 100 kN.

Table SI 1. Thermodynamic cycle analysis input and output parameters at design point

Cycle input parameters							
	Jet-A	100% SPK	LH_2	LNG	LNH_3	Methanol	Ethanol
Fan pressure ratio				1.6			
Fan polytropic efficiency				0.9			
Compressor pressure ratio				18			
Compressor polytropic efficiency				0.9			
Ambient or engine inlet pressure (Pa)				101,325			
Ambient or engine inlet temperature (K)				288			
Turbine polytropic efficiency				0.9			
Bypass ratio				5			
Heat capacity ratio at engine cold sections				1.4			
Specific heat capacity (constant pressure) at engine cold sections (J/kg)				1,005			
Heat capacity ratio at engine hot sections*	1.313	1.313	1.316	1.314	1.314	1.311	1.311
Specific heat capacity (constant pressure) at engine hot sections (J/kg)*	1212.14	1212.14	1243.09	1221.32	1251.69	1229.21	1229.21
Air to fuel ratio	50.00	51.04	138.89	57.87	21.53	23.03	31.48
Gas constant of combustion products (J/kg-K)*	289.04	289.04	298.21	291.58	299.31	291.78	291.78
Lower calorific value (MJ/kg)**	43.2	44.1	120.0	50.0	18.6	19.9	27.2
Fuel flow rate (kg/s)	0.89	0.88	0.31	0.77	2.01	1.92	1.40
Cycle output							
Thrust (kN)				100			
*source [85], ** source [2], [13]							

SI 4. Thermodynamic cycle analysis of a turbofan engine

SI 4.1 Overall efficiency and lost-fuel factors

Overall efficiency:

Table SI 2 lists the properties of different alternative fuels that are considered in this study. The ratios of fuel consumption rate of Jet-A fuel and fuel consumption rate of a given fuel ($\dot{m}_{\mathrm{f,Jet-A}}/\ \dot{m}_{\mathrm{f}}$) for Jet-A, 100% SPK, LH_2 and LNG are calculated at engine design point using GasTurb 13 software. An overview of GasTurb 13 software for cycle design and optimization is provided in SI §2. A turbofan engine in GasTurb 13 is operated for same thrust production (equal to Jet-A) at typical cruise altitude and Mach (35,000 ft [10.67 km] at Mach 0.85) using 100% SPK, LH_2, and LNG (separately), and the said ratios are calculated. Additionally, for LH_2 this ratio is also known from literature [86]. Ethanol, methanol and LNH_3 are unavailable fuels in GasTurb 13 software. For methanol and LNH_3 the said ratios are known from literature [85]. The ratio $\dot{m}_{\mathrm{f,Jet-A}}/\ \dot{m}_{\mathrm{f}}$ is not known for ethanol from literature. This ratio is calculated for ethanol as described below after assuming the ratio of overall efficiency for a given fuel case and overall efficiency for Jet-A ($\eta_{\mathrm{o,f}}/\ \eta_{\mathrm{o,Jet\text{-}A}}$). η_{o} is defined as the ratio of the propulsive power (product of thrust and velocity) to the fuel power ($\dot{m}_{\mathrm{f}}h_{\mathrm{f}}$) [87]. It is assumed that the thrust production and flight speed remain same for all fuel cases. The ratio $\eta_{\mathrm{o,f}}/\ \eta_{\mathrm{o,Jet\text{-}A}}$ = $\left(\dot{m}_{\mathrm{f,Jet-A}}h_{\mathrm{Jet-A}}\right)/\ (\dot{m}_{\mathrm{f}}h_{\mathrm{f}})$, for same thrust production and flight speed. Except for ethanol, this ratio is calculated from the known values and are listed in Table SI 2. The value of h for ethanol is greater than that for methanol but less than h of Jet-A. The ratio $\eta_{\mathrm{o,f}}/\ \eta_{\mathrm{o,Jet\text{-}A}}$ increases from 0.9993 (methanol) to 1 (Jet-A). Therefore, for ethanol this ratio must be between 99.93% and 100%. A value of 99.95% is assumed and the ratio $\dot{m}_{\mathrm{f,Jet-A}}/\ \dot{m}_{\mathrm{f}}$ is calculated for ethanol to be 0.63 as listed in Table SI 2. The η_{o} for the aircraft (Jet-A) considered in this research is considered in SI §4.4. Knowing this and the $\eta_{\mathrm{o,f}}/\ \eta_{\mathrm{o,Jet\text{-}A}}$ ratio for all fuels, the η_{o} is calculated

for all alternative fuels to be used on the said aircraft. We further conduct a sanity check on the ratio $\dot{m}_{\mathrm{f,Jet-A}}/\dot{m}_{\mathrm{f}}$ for all alternative fuels, that is calculated by using the above approach, using a simple thermodynamic cycle analysis of a turbofan engine (further details in SI §3). We observe that the ratio $\dot{m}_{\mathrm{f,Jet-A}}/\dot{m}_{\mathrm{f}}$ for all alternative fuels that calculated using both methods are similar.

Table SI 2. Properties of different alternative fuels

Fuel	h (MJ/kg)	Density ρ (kg/m^3)	$\dot{m}_{f,Jet-A}/\dot{m}_f$	$\eta_{\mathrm{o,f}}/\eta_{\mathrm{o,Jet\text{-}A}}$ (%)
Jet-A	43.2[1]	808[1]	1.00	100.00
100% SPK	44.1[2]	757[2]	1.02 *	99.97
LH_2	120.0[1]	71[1]	2.86 *,[3]	103.14
LNG	50.0[1]	424[1]	1.16 *	100.42
LNH_3	18.6[1]	730[1]	0.40[4]	92.90
Methanol	19.9[1]	796[1]	0.46[4]	99.93
Ethanol	27.2[1]	794[1]	0.63 ***	99.95 **

* Calculated using GasTurb 13
** is assumed value and *** is calculated based on it
[1] [2], [2] [13], [3] [86], [4] [85]

Lost fuel factor:

Equation 1 (in paper) estimates the aircraft range and we quantify the fuel consumed in non-cruise phases using the lost fuel factor, which represents a percentage of the GTOW and varies for different fuels [88], [89]. The lost fuel factor for Jet-A and LH_2 fuel is 2.2% and 1.4% of the GTOW of the aircraft [88], [89], respectively. Using the findings listed in Table SI 2, the lost fuel factor for other alternative fuels is calculated as a percentage of the (same) MTOW. For example, the MTOW of the Airbus A350-1000 aircraft is 316 tonnes. The lost fuel factors for other alternative fuels are listed in Table SI 3. Using the lost fuel factor of 2.2% of MTOW (316 tonnes for the A350-1000) Jet-A aircraft, the lost fuel is calculated (to be 6,952 kg). For the same period of operation, $\dot{m}_{\mathrm{f,Jet-A}}/\dot{m}_{\mathrm{f}}$ calculated in Table SI 2 equals $M_{\mathrm{f,Jet\text{-}A}}/M_{\mathrm{f}}$ listed in Table SI 3. Knowing $M_{\mathrm{f,Jet\text{-}A}}/M_{\mathrm{f}}$ ratios for other alternative fuels and $M_{\mathrm{f,Jet\text{-}A}}$ (6,952

kg) for Jet-A, the M_f for each of these alternative fuels is calculated. The lost fuel for each alternative fuel is then listed as a percent of the MTOW (316 tonne). As can be observed from Table SI 3, the alternative fuels with gravimetric energy densities lesser than Jet-A, such as LNH_3, methanol and ethanol have higher lost fuel factor i.e. more of the respective fuel is consumed. This is an expected trend.

Table SI 3. Lost fuel factor for alternative fuels

Fuel	$M_{f,Jet\text{-}A}$ / M_f	Lost fuel (kg)	% of MTOW (lost fuel)
Jet-A	1	6,952	2.20*
100% SPK	1.02	6,812	2.16
LNG	1.16	5,981	1.89
LNH_3	0.40	17,380	5.5
Methanol	0.46	15,103	4.78
Ethanol	0.63	11,041	3.49
* [88], [89]			

SI 4.2 Aerodynamics and additional fuselage structure

L/D ratio:

The drag coefficient (C_D) is estimated using equation SI 1, assuming that it is the sum of the zero-lift drag coefficient and lift-induced drag coefficient and that there is no wave drag,

$$C_D = C_{D,0} + \frac{C_L^2}{\pi\, AR\, e}, \quad \text{(SI 1)}$$

$$\text{where } C_{D,0} = \frac{C_f\, S_{wet}}{S}, \text{ and} \quad \text{(SI 2)}$$

$$C_L = \frac{W_{aircraft}}{0.5\, \rho_a\, S\, V^2}\ . \quad \text{(SI 3)}$$

$C_{D,0}$ is the coefficient of zero-lift drag, C_L is the coefficient of lift, AR (see SI §4.4), and e is the Oswald's efficiency factor, a correction factor that is representative of change in drag with lift of a 3D wing in comparison with an ideal wing that has same AR with an elliptical lift

distribution. An LTA aircraft such as the B777 has an 'e' value of 0.85 and this is used in the present study for the baseline aircraft [90]. C_f is the skin friction coefficient, which for today's large transport jets is typically 0.003 [91], [92]. S is the wing area known from aircraft data (see SI §4.4). The wetted area (S_{wet}) is calculated separately using the model described in the next section. Assumed values for the airspeed (V) and air density (ρ_a) are known from aircraft data (see SI §4.4). $W_{aircraft}$ is the aircraft weight at cruise, calculated as the average of the weight at the start and end of cruise. The wave drag modelling is a high order or high-fidelity analysis, which is beyond the scope of this work. For a present-day long-range sub-sonic aircraft like B787, the contribution of the wave drag (compressibility effects) to the total drag is small (2.9% at cruise altitude of 37,000 ft and Mach 0.85) [93]. After both C_L and C_D are calculated, the *L/D* (C_L/C_D) is calculated for cruise.

Wetted area and fuselage weight prediction model:

Aircraft wetted area prediction:

As observed from equations SI 1 and SI 2, S_{wet} is required for estimating the C_D. For a tube-wing aircraft, S_{wet} is calculated from using an empirical equation from Roskam [94] that relates S_{wet} to GTOW,

$$\log_{10}(S_{wet}\ [\text{ft}^2]) = D \log_{10}(\text{GTOW}\ [\text{lb}]) + C\ , \qquad \text{(SI 4)}$$

where the coefficients C and D are 0.0199 and 0.7531 respectively, for transport jets [94]. A validation of equation SI 4 is conducted for two cases, a Boeing 787 [93] and a tube-wing aircraft of future [95] , and gives agreement to within ±5% (< + 2%) (SI §7.1).

Fuselage wetted area and weight prediction:

For alternative fuels that are being studied here, a fraction of (for non-cryogenic fuels) or the entire fuel tanks (for cryogenic fuels) are installed in the fuselage. The increase in the fuselage length increases the aircraft wetted area, drag and weight, and resultantly the fuel consumption. Therefore, the S_{wet} of the alternative fuel powered aircraft is the sum of the S_{wet} of baseline aircraft and the wetted area of the additional fuselage required to store the alternative fuel. The fuselage wetted area ($S_{\text{wet,Fuselage}}$) is calculated as [96],

$$S_{\text{wet,Fuselage}}\,[\text{ft}^2] = \pi\, d_{\text{F}}\, l_{\text{F}} \left(1 - \frac{2\, d_{\text{F}}}{l_{\text{F}}}\right)^{\frac{2}{3}} \left(1 + \left(\frac{d_{\text{F}}}{l_{\text{F}}}\right)^2\right), \tag{SI 5}$$

where the parameters d_{F} and l_{F} represent the cylindrical fuselage diameter and length (in ft). The fuselage weight (W_{Fuselage}) is then calculated as [97], [98],

$$W_{\text{Fuselage}}[\text{lb}] = 5\ S_{\text{wet,Fuselage}}\,[\text{ft}^2]. \tag{SI 6}$$

Validation of equations SI 5 and SI 6 is included in the SI §7.2, where $S_{\text{wet,Fuselage}}$ and W_{Fuselage} of a Boeing 787 predicted using this method are within ±5% of their known values.

SI 4.3 Additional systems weight for alternative fuels

In all cases of alternative fuels studied here, the OEW of the aircraft is expected to change as a result of the need for additional fuel storage, or fuel tank systems and the structure required to support these tank systems. The additional fuselage length for all alternative fuels is estimated from the fuel volume that need to be stored in the fuselage tanks.

Non-cryogenic fuels:

For non-cryogenic fuels, a substantial fraction of the $W_{\text{F,total}}$ fits inside the existing tanks in the wings based on the tank volume of the baseline aircraft. The remainder of the fuel must be accommodated in the (additional) fuselage. There are two components of additional weight

considered for non-cryogenic fuels: the additional tank weight required to hold the remaining fuel that cannot fit in the wing tanks and the additional fuselage weight required to accommodate this additional tank. The additional fuselage weight is calculated according to the approach described in SI §4.2.

To estimate the additional tank weight for non-cryogenic fuels that have similar mass densities as Jet-A (100% SPK, ethanol, and methanol), we use the findings of Goraj [99], who reported that the structural weight of a conventional fuel tank is ~1/70 of the fuel weight. Thus, the OEW calculation for non-cryogenic fuels ($\mathrm{OEW}_{\mathrm{non-cryogenic}}$) is given by,

$$\begin{aligned}\mathrm{OEW}_{\mathrm{non-cryogenic}} &= \mathrm{OEW}_{\mathrm{baseline}}(1-\omega) \\ &+ \frac{1}{70}\left(W_{\mathrm{F,total,non-cryogenic}} - \frac{\rho_{\mathrm{non-cryogenic}}\ W_{\mathrm{F,total,baseline}}}{\rho_{\mathrm{Jet-A}}}\right) \\ &+ \left(W_{\mathrm{Fuselage,non-cryogenic}} - W_{\mathrm{Fuselage,baseline}}\right)(1-\omega),\end{aligned} \quad \text{(SI 7)}$$

where $W_{\mathrm{F,total,non-cryogenic}}$ and $W_{\mathrm{F,total,baseline}}$ are the total fuel weights of the non-cryogenic fuel and Jet-A fuel respectively at mission start; $\rho_{\mathrm{non-cryogenic}}$ and $\rho_{\mathrm{Jet-A}}$ are the densities of the non-cryogenic fuel and Jet-A fuel respectively; and $W_{\mathrm{Fuselage,non-cryogenic}}$ is the fuselage weight of the non-cryogenic aircraft. ω is the weight reduction factor for fuselage weight and OEW (in percentage), which is dependent on technology improvement. We set it to zero by default for all non-cryogenic fuel cases during the performance evaluation of different alternative liquid fuels considered in this work.

Cryogenic fuels:

For cryogenic fuels (LH_2, LNG and LNH_3), in addition to the additional fuselage weight we also add the weight of cryogenic tank systems and structural weight added to support the cryogenic tank system to the OEW of the aircraft.

The gravimetric index, gravimetric efficiency or gravimetric storage density (η), defined as the ratio of cryogenic fuel weight to the sum of the dry tank weight and cryogenic fuel weight [20], [86], [100], [101]. The tank weight is dependent on the type of the insulation system used in its design [26]. Therefore, η is an important technology parameter that determines the feasibility of cryogenic-fuelled aircraft [100]. Advances in lighter and stronger composite materials have recently shown LH_2 cryogenic tank $\eta = 0.92$ for manufactured tanks [102] (which could improve in future), and that too for a small size tank (diameter 1.2 m and length 2.4 m). A study by Sjöberg et al. [103] models a light weight LH_2 tank (4.7 m length and 3 m diameter) using composite materials with $\eta = 0.94$ for a full tank, in comparison with metallic tank having $\eta = 0.71$. For the LH_2 fuel case in the present work, an integral type of cryogenic tank with foam-based insulation is selected in this study. An average value of η of 0.78 for long-range LH_2 aircraft is selected with an insulation thickness of 8.1 cm according to the study by Verstraete et al. [20]. We acknowledge that there is significant uncertainty in the value of η; for example, foam based integral tanks are known to have higher η compared to other tank types, especially for larger tank volumes (on the order of 75%) [20], whereas a value of $\eta = 0.38$ was assumed to represent a double-wall evacuated tank with multi-layer insulation for a large long-range aircraft by the Clean Sky 2 - Fuel Cells and Hydrogen (FCH) joint project [100], [104]. In this study, we use an optimistic value and will explore the sensitivity due to this uncertainty in future work. For LNG, two cases are analysed, where the fuel tank is integral to the fuselage structure. The first LNG case uses a hypothetical value of $\eta = 0.78$, like LH_2 case. In the second LNG case, a present-day (best) value of $\eta = 0.63$ is used, which is similar to the values used in transportation of LNG fuel via trucks [105]. For LNH_3, the fuel the tank is assumed to be integral to the fuselage structure. The weight of cryogenic tank (assumed to be made of steel) is a quarter of the weight of required fuel (or $\eta = 0.8$) as a thumb rule according to Dincer et al. [106]. To calculate the tank internal volume, with the

outer diameter constrained by the fuselage diameter, we assume that the insulation thickness of 8.1 cm that we use for the LH_2 case [20] is also applicable to the LNH_3 and LNG cases.

For all three cryogenic fuels (LH_2, LNG and LNH_3) to be installed in the fuselage, a structural support weight for the integral cryogenic tanks is added which is 6% of the fuselage weight according to the study by Verstraete et al. [20]. While this weight penalty was defined for a LH_2 aircraft, we assume that the same penalty applies to both LNG and LNH_3 aircraft since there are less published studies on these fuels. Therefore, the OEW calculation for cryogenic fuels is,

$$\begin{aligned} \mathrm{OEW}_{\mathrm{cryogenic}} = \mathrm{OEW}_{\mathrm{baseline}}\,(1-\omega) + \frac{(1-\eta)\;W_{\mathrm{F,total,cryogenic}}}{\eta} \\ + 0.06\,W_{\mathrm{Fuselage,baseline}}(1-\omega) \\ + \left(W_{\mathrm{Fuselage,cryogenic}} - W_{\mathrm{Fuselage,baseline}}\right)(1-\omega), \end{aligned} \tag{SI 8}$$

where $\mathrm{OEW}_{\mathrm{baseline}}$ is the baseline aircraft OEW, $W_{\mathrm{F,total,cryogenic}}$ is the total fuel weight of the cryogenic fuel at mission start, and $W_{\mathrm{Fuselage,cryogenic}}$ and $W_{\mathrm{Fuselage,baseline}}$ are the fuselage weight of the cryogenic and baseline aircraft respectively. ω is dependent on technology improvement and it is zero by default for all cryogenic fuel cases in this study.

SI 4.4 Known and calculated aircraft data

The Airbus A350-1000 aircraft is chosen as the baseline aircraft for the comparative assessment of the performance characteristics of the 100% SPK, LH_2, LNG, LNH_3, ethanol and methanol in comparison with the performance of Jet-A. Table SI 4 lists the A350-1000 aircraft data which will be used for the aircraft performance modelling using Breguet's range equation. The η_o for the A350-1000 aircraft (Jet-A) is known to be 0.4. Knowing this and the $\eta_{o,f}/\,\eta_{o,\text{Jet-A}}$ ratio for all fuels (known from SI §4.1), the η_o is calculated for all alternative fuels to be used on the aircraft.

Table SI 4. Aircraft data (Airbus A350-1000 Jet-A) and cruise conditions

Parameters	Units	Value
Aircraft data (Airbus A350-1000)		
Maximum take-off weight (MTOW)	kg	316,000[1]
Maximum PAX in a 3-class configuration	-	366[1]
Average weight of one passenger	kg	95[1], [2]
Passenger payload weight (W_p)	kg	34,770 (= 366 x 95)
Total fuel weight ($W_{F,total, Jet-A}$) at mission start	kg	126,101[1]
Operating empty weight ($OEW_{Baseline}$) (= MTOW – $W_{F,total, Jet-A}$ – W_p)	kg	155,129
Overall efficiency (η_o)	-	0.4[3]
Fuselage length (l_f)	m	72.25[1]
Fuselage width (d_f)	m	5.96[1]
Fuselage fineness ratio (l_f/d_f)	-	12.12
Wing area	m^2	465[4], [5]
Span	m	65[1]
Aspect ratio AR (= $span^2$/wing area)	-	9.12
Typical cruise conditions for large transport jets		
Altitude	ft	35,000
	m	10,668
Airspeed at 35,000 ft (10,668 m)	knots	490[6]
	m/s	252.1
Mach number	-	0.85[6]
Air density ρ_a at 35,000 ft	kg/m^3	0.38 [7]
Calculated data		
$S_{wet,Fuselage}$	m^2	1,208
	ft^2	13,000
$W_{Fuselage}$	kg	29,484 kg
$S_{wet,Fuselage}$	m^2	2,445
	ft^2	26,320

[1] [107], [2] [108],
[3] [109],
[4] [110], [5] [111], [6] [112] [7] [113]

SI 5. Stepwise procedure of the range equation analysis for Jet-A (baseline) case and alternative fuel cases at design point

SI 5.1 Conventional jet fuel (Jet-A) case

The methodology description in §2 of the paper is listed/summarized below as a stepwise process of the range equation analysis for Jet-A (baseline) case (based on Figure 1 in the paper):

- Step 1: Use the known values of OEW, W_p, $W_{F,total}$ of the aircraft to estimate the aircraft GTOW (= OEW + $W_{F,total}$ + W_p).
- Step 2: Input the known lost fuel value, h and η_o, for Jet-A aircraft being evaluated.
- Step 3: Calculate $W_{initial}$ and W_{final}

  $W_{initial}$ = (1 – lost fuel value) x GTOW

  W_{final} = GTOW – 0.9 x $W_{F,total}$
- Step 4: Calculate the aircraft L/D
- Step 5: Calculate the Jet-A aircraft range using Breguet's range equation (equation 1)

SI 5.2 Alternative cryogenic fuel cases

For alternative cryogenic fuel cases (based on Figure 2 in the paper), the description in §2 of the paper is listed/summarized below as a stepwise process of the range equation analysis:

- Step 1: Guess a value (initial guess value of 1 kg) for $W_{F,total}$
- Step 2: The OEW for the alternative cryogenic fuel case is calculated based on the value of $W_{F,total}$ as additional fuselage structure is required to store the said fuel in cryogenic tanks.
- Step 3: The GTOW (= OEW + $W_{F,total}$ + W_p) is calculated for a given payload case
- Step 4: Is the GTOW<=MTOW of the aircraft?

- Step 5: If ‘yes’ to question in step 4, estimate the lost fuel value, h and η_o , for the alternative fuelled aircraft under consideration.
- Step 6: After step 5, calculate $W_{initial}$ and W_{final}

  $W_{initial}$ = (1 – lost fuel value) x GTOW

  W_{final} = GTOW – 0.9 x $W_{F,total}$
- Step 7: After step 6, calculate the aircraft *L/D* (includes penalty due to additional fuselage requirement)
- Step 8: After step 7, calculate the aircraft range using Breguet’s range equation (equation 1)
- Step 9: Does the calculated range of the alternative fuelled aircraft meet the target range of the Jet-A (baseline) aircraft?
- Step 10: If ‘yes’ to the question in step 9, then the aircraft is fixed/finalized
- Step 11: If ‘no’ to the question in step 9, then increase the guess for $W_{F,total}$ and execute step 1 to follow the steps thereafter
- Step 12: If ‘no’ to question in step 4, then restore values of all parameters from previous iteration (based on previous guess of $W_{F,total}$), and the aircraft is fixed/finalized.

SI 5.3 Alternative non-cryogenic fuel cases

For alternative non-cryogenic fuel cases (based on Figure 2 in the paper), the description in §2 of the paper is listed/summarized below as a stepwise process of the range equation analysis:

- Step 1: Guess a value (initial guess value of 1 kg) for $W_{F,total}$
- Step 2: Does total fuel at mission start fit inside the wing tanks?
- Step 3: If ‘yes’ to question in step 2, the OEW of aircraft is same as that of the Jet-A aircraft case i.e. no additional fuselage.

- Step 4: If ‘no’ to question in step 2, estimate (and store) the fuel volume that fits inside the wing tanks and for the remaining fuel (calculate the) additional fuselage is required for storing non-cryogenic fuel tank. The OEW of aircraft is calculated based on this additional fuselage requirement.
- Step 5: Following step 3 or 4, the OEW for the alternative non-cryogenic fuel case is calculated.
- Step 6: The GTOW (= OEW + $W_{F,total}$ + W_p) is calculated for a given payload case
- Step 7: Is the GTOW<=MTOW of the aircraft?
- Step 8: If ‘yes’ to question in step 7, estimate the lost fuel value, h and η_o , for the alternative fuelled aircraft under consideration.
- Step 9: After step 7, calculate $W_{initial}$ and W_{final}

  $W_{initial}$ = (1 – lost fuel value) x GTOW

  W_{final} = GTOW – 0.9 x $W_{F,total}$
- Step 10: After step 9, calculate the aircraft L/D (includes penalty due to additional fuselage requirement)
- Step 11: After step 10, calculate the aircraft range using Breguet’s range equation (equation 1)
- Step 12: Does the calculated range of the alternative fuelled aircraft meet the target range of the Jet-A (baseline) aircraft?
- Step 13: If ‘yes’ to the question in step 12, then the aircraft is fixed/finalized
- Step 14: If ‘no’ to the question in step 12, then increase the guess for $W_{F,total}$ and execute step 1 to follow the steps thereafter
- Step 15: If ‘no’ to question in step 7, then restore values of all parameters from previous iteration (based on previous guess of $W_{F,total}$), and the aircraft is fixed/finalized.

SI 6. Stepwise procedure of the range equation analysis at off-design point

SI 6.1 Maximum permissible range estimation with full fuel tank

The stepwise process shown in Figure 3 in the paper is as follows:

- Step 1: Use the fixed/designed aircraft where values of OEW, maximum $W_{F,total}$ and maximum payload weight are known for fuel under consideration. Begin with full fuel tank capacity for a given payload case (weight) within the maximum payload limit and estimate the aircraft GTOW (= OEW + $W_{F,total}$ (max.) + W_p).
- Step 2: Input the known lost fuel value, h and η_o, for aircraft and fuel being evaluated.
- Step 3: Calculate $W_{initial}$ and W_{final}

  $W_{initial}$ = (1 – lost fuel value) x GTOW

  W_{final} = GTOW – 0.9 x $W_{F,total}$
- Step 4: Calculate the aircraft L/D
- Step 5: Calculate and record the aircraft range using Breguet's range equation (equation 1) with full fuel tank capacity for a given payload case (weight). This is the maximum permissible range for given payload case (with full fuel tank capacity).

SI 6.2 Estimation of block energy consumption for given range and payload combination

The stepwise process shown in Figure 4 in the paper is as follows:

- Step 1: Use the fixed/designed aircraft where values of OEW, maximum $W_{F,total}$ and maximum payload weight are known for fuel under consideration. For a given payload case (weight) within the maximum payload limit, select the aircraft range at which fuel performance needs to be evaluated (example: 5000 km). This range selection should be

within maximum range of aircraft for given payload, which is evaluated using schematic shown in Figure 3.

- Step 2: Begin with a guess value (initial guess value of 1 kg) for $W_{F,total}$.
- Step 3: The GTOW (= OEW + $W_{F,total}$ + W_p) is calculated for a given payload case
- Step 4: Use the lost fuel value, h and η_o, for the fuel case under consideration.
- Step 5: Calculate $W_{initial}$ and W_{final}

  $W_{initial}$ = (1 – lost fuel value) x GTOW

  W_{final} = GTOW – 0.9 x $W_{F,total}$
- Step 6: Calculate the aircraft L/D
- Step 7: Calculate the aircraft range using Breguet's range equation (equation 1)
- Step 8: Does the calculated range of the aircraft meet the target (selected range) range (example: 5000 km considered in step 1)?
- Step 9: If 'yes' to the question in step 8, then record the block fuel/energy consumption for given range and payload combination

  Block fuel consumption = 0.9 x $W_{F,total}$ (as discussed in sub-section 4.3.1)
- Step 10: If 'no' to the question in step 8, then increase the guess within the maximum value of total fuel weight at mission start for given aircraft-fuel case and execute step 2 to follow the steps thereafter.

SI 7. Validation of the used equations

SI 7.1 Validation of aircraft wetted area prediction equation

The aircraft wetted area (S_{wet}) prediction equation needs to be tested for its accuracy while predicting S_{wet} of recent or advanced/NextGen tube-wing aircraft. Two validation cases are conducted here. According to the book by Kundu et al. [114] and thesis of Kirby [115], a prediction difference of ±5% is an acceptable/typical industry trend in the conceptual design phase or for low-order modelling. The above criteria of ±5% prediction difference is used for establishing confidence in the model. The first case is S_{wet} estimation of Boeing 787-8 aircraft. Piano-X is an aircraft analysis tool and PIANO-X data for this aircraft with take-off weight of 476,000 lb (215,910 kg) estimates the S_{wet} to be 19,533 ft^2 (1815 m^2) [93]. Substituting the take-off weight of 476,000 lb in equation SI 4 (S_{wet} prediction equation in SI §4.2), S_{wet} is calculated to be 19,756 ft^2 (1835 m^2), compared to the S_{wet} estimate of 19,533 ft^2 known from PIANO-X data. The prediction difference between PIANO-X data and prediction by using equation SI 4 is +1.14%. The second case is S_{wet} estimation of an advanced tube-wing aircraft. The study by Nickol et al. [95] designs an advanced tube-wing aircraft for seating 300 passengers using FLOPS software. The GTOW of this aircraft is 503,350 lb (228,316 kg). Substituting this GTOW in equation SI 4, S_{wet} is calculated to be 20,605 ft^2 (1914 m^2) compared to the wetted area estimation of 20,600 ft^2 by Nickol et al. study. The Roskam's model is found to be highly accurate as the prediction difference is +0.024%. For both cases, the Roskam's model is found to be accurate with a prediction difference well within the criteria defined (prediction difference of ±5%) for accuracy during the conceptual design phase or low-order modelling.

SI 7.2 Validation of fuselage wetted area and weight prediction equation

Before using equation SI 5 (fuselage wetted area [$S_{\text{wet, Fuselage}}$] prediction equation) and equation SI 6 (fuselage weight [W_{Fuselage}] prediction equation) from SI §4.2, these need to be tested for their accuracy using the above defined criteria. Piano-X data for B787-8 aircraft estimates $S_{\text{wet, Fuselage}}$ of 9,484 ft^2 (881 m^2) and 'fuselage group weight' of 44,917 lb (20,374 kg) [93]. For B787-8 aircraft, the values of fuselage diameter d_f and fuselage length l_f are 18.83 ft and 183.5 ft respectively [93]. Substituting these values of d_f and l_f in equation SI 5, the $S_{\text{wet, Fuselage}}$ is calculated to be 9,412 ft^2 (874 m^2), compared to the $S_{\text{wet, Fuselage}}$ value of 9,484 ft^2 from Piano-X (prediction difference of -0.76%). Substituting this predicted $S_{\text{wet, Fuselage}}$ of 9,412 ft^2 in equation SI 6, results in W_{Fuselage} of 47,060 lb (21,346 kg) compared to the 'fuselage group weight' of 44,917 lb from Piano-X (prediction difference of +4.77%). The prediction difference by the use of equation SI 5 and equation SI 6 are within the criteria defined (prediction difference of ±5%) for accuracy during the conceptual design phase or low-order modelling.

SI 7.3 Validation of Breguet's range equation

Two aircraft are considered for validation of Breguet's range equation. Each aircraft has two operational points of range and payload combinations. Overall, there are four validation points. Additionally, the lift to drag ratio estimation, which is an intermediate calculation step, is also validated for both aircraft. The two aircraft considered here are Airbus A320-200 and Boeing 767-300F. The A320-200 is a small narrow-body and single-aisle aircraft and the B767-300F is a small wide-body freighter aircraft. It is to be noted that both aircraft are small transport jets. The skin friction coefficient (C_f) for small transport jets is 0.0035 [91], in comparison with 0.003 for large transport jet (used in SI §4.2). Table SI 5 and Table SI 6 below provide the characteristics of Airbus A320-200 and Boeing 767-300F aircraft respectively that are required for Breguet's range equation analysis.

Table SI 5. Airbus A320-200 aircraft characteristics

Parameter	Units	Value	Reference
OEW	kg	44,200	[116]
MTOW	kg	73,500	[116]
Maximum payload	kg	16,565	[116]
Range at maximum payload	km	2,935	[116]
	nmi	1,585	[116]
Payload at maximum range	kg	10,341	[116]
Maximum range	km	5,181	[116]
	nmi	2,798	[116]
Cruise *L/D*	-	15 – 16	[117]
Overall efficiency	-	0.3	Calculated using [117]
Wing area	m^2 or ft^2	122.4 or 1,317.5	[118], [119]
Aspect ratio	-	9.5	[118], [119]
Cruise Mach	-	0.795	[118], [119]
Cruise altitude	ft or km	37,000 or 11.28	[118], [119]
Air density at cruise altitude	kg/m^3	0.348	Calculated using [120]
Speed of sound at cruise altitude	m/s	295.07	Calculated using [120]

For the A320-200 aircraft, overall efficiency η_o is not known directly. However, the cruise thrust specific fuel consumption (TSFC) of this aircraft is known to be ~17.5 mg/N-s from resource [121]. Using the definition of η_o,[flight speed/(TSFC x LCV)] its value is estimated. The flight speed in cruise is 234 m/s [= 0.8 (Mach) x 295.54 (speed of sound)]. The η_o is estimated to be 0.3 for A320-200 aircraft (as listed in Table SI 5). Additionally, the cruise *L/D* for A320-200 is known to be (approximately) 15 – 16 [117]. The cruise *L/D* is plotted in a figure in resource [117], and so the exact value is not known. This approximate value of cruise *L/D* for A320-200 listed in Table SI 5.

Table SI 6. Boeing 767-300F aircraft characteristics

Parameter	Units	Value	Source
MTOW	kg	185,065	[122]
Maximum zero fuel weight (MZFW)	kg	140,160	[122]
Maximum payload (PL_{max})	kg	52,700	[123]
OEW (= MZFW - PL_{max})	kg	87,460	Calculated
Range with 40,823 kg payload	km	7,408	[122]
	nmi	4,000	[122]
Range with 50,800 kg payload	km	5,556	[122]
	nmi	3,000	[122]
Cruise *L/D*	-	15-16	Estimated using [121]
Overall efficiency (η_o)	-	0.34	Estimated using [109], [124]
Wing area	m^2 or ft^2	282.3 or 3,050	[125]
Aspect ratio	-	7.99	[125]
Cruise Mach	-	0.8	[123]
Cruise altitude	ft or km	35,000 or 10.67	[123]
Air density at cruise altitude	kg/m^3	0.38	Calculated using [120]
Speed of sound at cruise altitude	m/s	296.54	Calculated using [120]

Table SI 7. Airbus A320-200 and Boeing 767-300F aircraft performance validation

Parameter	Published	Calculated in this study	Prediction difference
Airbus A320-200			
Range with 16,565 kg payload (1)	2,935 km	3,054 km	+4.05%
L/D for (1)	15-16*	15.7	-

Range with 10,341 kg payload (2)	5,181 km	4,947	-4.52%
L/D for (2)	15-16*	15.48	-
Boeing 767-300F			
Range with 40,823 kg payload (3)	7,408 km	7,098 km	-4.19
L/D for (3)	15-16*	15.75	-
Range with 50,800 kg payload (4)	5,556 km	5,604	+0.86%
L/D for (4)	15-16*	15.86	-

* Typical cruise *L/D*

Similarly, for the B767-300F aircraft, η_o is not known directly. However, the η_o of Boeing 747-400 aircraft is known to be ~0.34 from resource [109]. The B747-400 aircraft uses four CF6 – 80C2 engines and B767-300F uses two CF6 – 80C2 engines [124]. Hence, the η_o of B767-300F aircraft is expected to be 0.34 and is listed in Table SI 6. Additionally, the cruise *L/D* for B767-300F is not known directly. However, the cruise *L/D* of similar size/type aircraft viz. Airbus A310 and B767-300ER are known to be about 15 – 16 from resource [117]. The cruise *L/D* is plotted in a figure in resource [117], and so the exact value is not known. This approximate value of cruise *L/D* (of 15 – 16) is expected to be same for B767-300F aircraft and this value is listed in Table SI 6. The required data for Breguet's range analysis of the above two aircraft are now known.

Table SI 7 lists the Airbus A320-200 and Boeing 767-300F aircraft performance validation. As discussed before, each aircraft has two operational points of range and payload combinations, and overall there are four validation points. It can be observed from Table SI 7 that Breguet's range equation for the estimation of range is accurate to within ±5%, which is acceptable for conceptual design phase or low-order modelling used in this work. Additionally,

the cruise *L/D* for both aircraft at each of the four points is in reasonable agreement with the published values.

SI 7.4 Validation of the LH_2 aircraft from the Clean Sky 2 – Fuel Cells and Hydrogen joint project

An attempt is made below to replicate the long-range LH_2 aircraft design in the Clean Sky 2 - Fuel Cells and Hydrogen (FCH) joint project [100], where very few/limited design details or aircraft characteristics are revealed.

Table SI 8. Comparison of LH_2 aircraft characteristics for passenger payload of 30,875 kg (325 passengers) between the Clean Sky 2 – FCH joint project and the present study

Fuel and study	Cryogenic tank η	Payload weight W_p (kg)	Fuselage length (m)	ΔL (m)	ΔL (%)	Range (km)
LH_2 (Clean Sky 2 – FCH joint project [100])	0.38	30,875	-	-	30.00	10,000
LH_2 (Using present model)	0.38	30,875	93.99	21.74	30.09	10,000

It is known from the project report that the long-range LH_2 aircraft from the Clean Sky 2 – FCH joint project seats 325 passengers and has a design range of 10,000 km, where the cryogenic tank η is 0.38 for an integral tank with double walled multi-layer insulation system [100], [104]. Using the model of the A350-1000 aircraft developed in the present work, an LH_2 powered large aircraft is designed for 325 passenger-payload (30,875 kg) with a target design range of 10,000 km and a cryogenic LH_2 tank η value of 0.38 is used. The aircraft performance characteristics of the said aircraft is listed in Table SI 8. It can be observed from Table SI 8 that the magnitude of increase in LH_2 aircraft fuselage length calculated in this work and the published value in Clean Sky 2 – FCH joint project are similar for the same cryogenic tank η and passenger payload.

SI 8. Results of the performance characteristics of aircraft powered by different fuels

SI 8.1 Miscellaneous results of the performance characteristics at design point

The performance characteristics of Airbus A350-1000 aircraft modified for the use of alternative fuels (for same payload of 34,770 kg i.e. 366 passenger payload) is listed in Table SI 9. ΔL in Table SI 9 represents the additional fuselage length for accommodating the alternative liquid fuel. The fuselage and aircraft modification data of Airbus A350-1000 aircraft for the use of alternative liquid fuels is listed in Table SI 10. It is to be noted that the wing planform (area, span and/or aspect ratio) is maintained constant for different fuel cases. This is similar to or in-line with the approach used in the Cryoplane study of minimal change to the wing planform, and the positive effects of this approach on the wing loading are observed later.

As discussed in SI §4.3, for LNG two cases are evaluated - the first LNG case uses a hypothetical (futuristic) η of 0.78 similar to LH_2 case and in the second LNG case a present-day value of η of 0.6274 is used which is similar to the values used in transportation of LNG fuel via trucks. The effect of LNG cryogenic tank η can be observed from Table SI 9. With increasing η, the aircraft range and $W_{F,total}$ increases, and the OEW decreases.

Table SI 9. Airbus A350-1000 performance characteristics using alternative liquid fuels for passenger payload of 34,770 kg (366 passengers) for same wing area (465 m^2) and aspect ratio (9.12)

Fuel	*h/g* (km)	Cryogenic tank η	OEW (kg)	$W_{F,total}$ (kg)	GTOW (kg)	Fuel in fuselage tank (kg)	ΔL (m)	*L/D*	*R* (km)
Jet-A	4,404	-	155,129	126,101	315,999	-	-	18.63	13,870
100% SPK	4,496	-	155,314	123,320	313,404	5,178	0.25	18.57	13,870
LH_2	12,233	0.78	183,371	50,375	268,516	50,375	26.87	16.09	13,870
LNG Case 1	5,097	0.78	187,239	93,990	315,999	93,990	8.40	18.20	10,895

LNG Case 2	5,097	0.63	205,161	76,068	315,999	76,068	6.77	18.48	8,517
LNH_3	1,896	0.80	183,605	97,624	315,999	97,624	5.05	18.34	3,478
Methanol	2,029	-	155,191	126,037	315,999	1,809	0.08	18.52	5,943
Ethanol	2,773	-	155,202	126,027	315,999	2,111	0.10	18.57	8,421

It can be observed from Table SI 9 that only 100% SPK and LH_2 powered aircraft are able to fly same range/distance (R) as that of the Jet-A aircraft (baseline) within the same limit of MTOW (of 316 tonne). Since other alternative fuels have lower h as compared to Jet-A, higher quantity of fuel would be required (to be carried) on the aircraft for enabling the same range as that of the Jet-A aircraft. This also increases the OEW of the aircraft and resultantly the GTOW. Since the GTOW is structurally limited by the MTOW bound, limited fuel and corresponding OEW can be supported for a given aircraft structure (MTOW defined).

It should be noted that since LH_2 has 2.78 times higher gravimetric energy density than Jet-A, $W_{F,total}$ for LH_2 is less than that for Jet-A. The lower volumetric energy density of LH_2 fuel increases the fuselage length by 26.87 m (or by 37.2%) compared to Jet-A case. This finding is similar to the observation made in the study by Verstraete [126] where there is 38.2% increase in fuselage length for a single-decker 300 passenger LH_2 aircraft (using similar cryogenic tank η) that has a design range of 9,000 km. In this work, the 37.2% increase in LH_2 aircraft fuselage length compared to Jet-A case, penalizes the aircraft performance as the LH_2 aircraft fuselage weight increases to 41,749 kg from 29,484 kg, and L/D ratio decreases to 16.09 from 18.63. The associated increase in fuselage wetted area and aircraft wetted area can be observed from Table SI 10.

Table SI 10. Airbus A350-1000 fuselage and aircraft modification data for different alternative fuels for passenger payload of 34,770 kg (366 passengers) for same wing area (465 m^2) and aspect ratio (9.12)

Fuel	l_f (m)	Fuselage structural weight $W_{Fuselage}$ (kg)	Fuselage wetted area $S_{wet,Fuselage}$ (m^2)	Aircraft wetted area S_{wet} (m^2)	Wing loading (kg/m^2)	SEC (MJ/tonne-km)
Jet A	72.25	29,484	1,208	2,445	679.6	10.17
100% SPK	72.5	29,596	1,212	2,450	674.0	10.15
LH_2	99.12	41,749	1,710	2,948	577.5	11.28
LNG C1	80.65	33,315	1,365	2,602	679.6	11.17
LNG C2	79.02	32,572	1,334	2,572	679.6	11.56
LNH_3	77.3	31,785	1,302	2,539	679.6	13.51
Methanol	72.33	29,521	1,209	2,447	679.6	10.93
Ethanol	72.35	29,527	1,210	2,447	679.6	10.54

In terms of absolute value, for a single decker 400 passenger aircraft with a design range of 14,000 km, the study by Verstraete [126] finds that the LH_2 aircraft (similar cryogenic tank η) fuselage length is greater than 95 m which is similar in magnitude to the finding of this work (of approximately 99 m). More design details of this single decker 400 passenger aircraft by Verstraete [126] are not known limiting further comparison.

The cryogenic tank η used by Brewer [34], [86], [127] ($\eta = 0.836$) is of the similar order used in this work ($\eta = 0.78$). According to the book by Brewer [127], the LH_2 aircraft will have lower wing loading. Brewer [34], [86], [127] evaluates a double-decker 400 passenger LH_2 aircraft (18,500 km range). The wing (area) is subjected to modifications (wing structural weight and loading). The wingspan and wing area reduces from 87.7 m (Jet-A) to 66.2 m (LH_2 fuel) and from 698.7 m^2 (Jet-A) to 438.1 m^2 (LH_2 fuel), respectively. The aspect ratio ($span^2$/ area) reduces from 11 (Jet-A) to 10 (LH_2 fuel). The gross take-off weight of the Jet-A and LH_2

aircraft are known to be 476,230 kg and 249,400 kg, respectively. The wing loading of the Jet-A and LH_2 aircraft are calculated to be (476,230 kg/698.7 m^2 =) 681.6 kg/m^2 and (249,400 kg/438.1 m^2 =) 569.3 kg/m^2, respectively. Therefore, the wing loading of the double-decker 400 passenger LH_2 aircraft (18,500 km range) evaluated by Brewer [127] reduces by 16.5%, compared to the baseline Jet-A aircraft. In the present work, the wing planform (area, span and/or aspect ratio) is maintained constant for different fuel cases. This is similar to or in-line with the approach used in the Cryoplane study of minimal change to the wing planform. As observed from Table SI 10, the wing-loading of the LH_2 aircraft (577.5 kg/m^2) modelled in this work reduces by 15% (similar to 16.5% reduction observed by Brewer), in comparison with the wing-loading of the Jet-A aircraft (679.6 kg/m^2).

For 100% SPK fuel, the extra fuel (in addition to the wing tank) required considering slightly lower volumetric energy density as compared to Jet-A, to meet the flight range of Jet-A aircraft within the MTOW limit of 316 tonne, is small as compared to the fuel that fits in the wing tanks. Therefore, for 100% SPK, ΔL is 0.25 m which has an insignificant impact on the (wetted area) *L/D* performance.

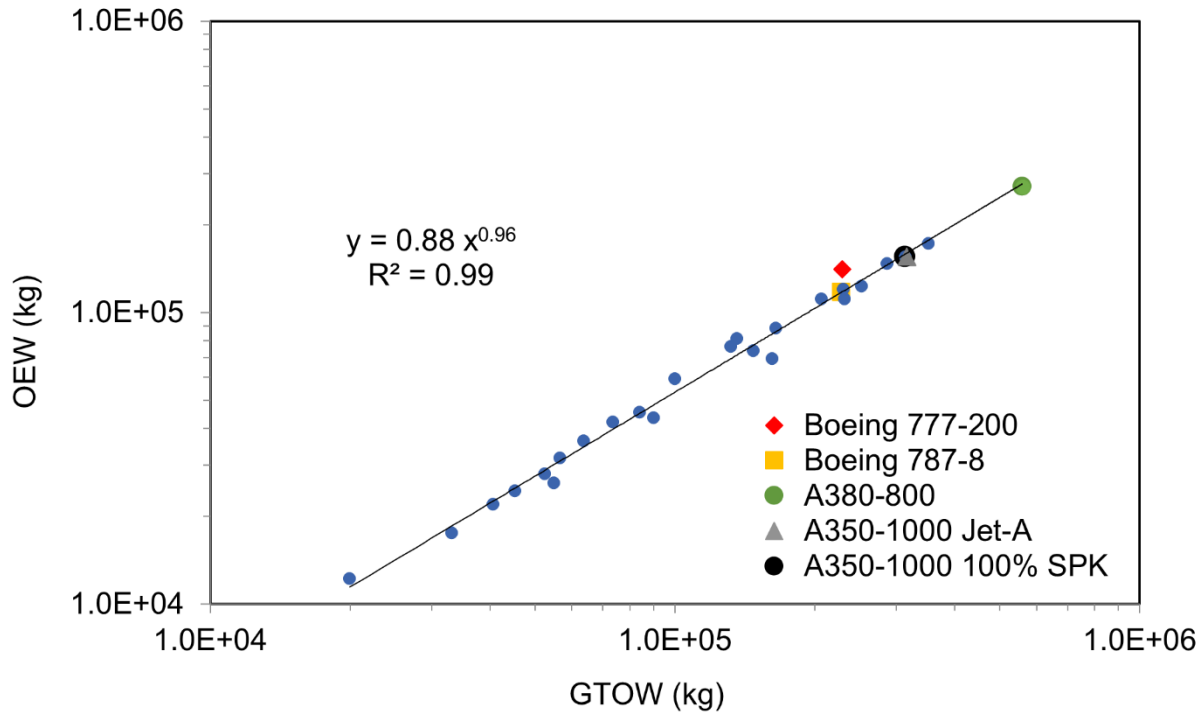

Figure SI 3. Relationship between OEW and GTOW of 100% SPK from the present study and aircraft in service for facilitating weight sizing studies

Figure SI 3 shows the relationship between OEW and GTOW of 100% SPK from the present study and aircraft in service. It can be observed that the relationship between OEW and GTOW for the aircraft designed in this research is similar to that of aircraft in service. 100% SPK aircraft have similar (magnitude of) OEW and GTOW as that of Jet-A case. For compactness, only the names of recent aircraft in service and the aircraft designed in this research are mentioned in Figure SI 3. The data points comprise of small and medium size aircraft, large twin aisle aircraft and large quad. All data points (OEW and GTOW data of aircraft in service and aircraft designed in this research), are listed in Table SI 11. Additionally, the developed equation is useful during preliminary design or aircraft weight sizing process, and knowing either OEW or GTOW, the GTOW or OEW can be estimated.

Table SI 11. OEW and GTOW data of aircraft in service and aircraft designed in this study [94], [128]

Aircraft	GTOW (kg)	OEW (kg)
727-200	83,824	45,359
737-200	52,390	27,955
737-300	56,472	31,720
747-200B	351,534	172,365
747-SP	285,763	147,417
757-200	99,790	59,157
767-200	136,078	81,230
DC8-Super 71	147,417	73,799
DC9-30	54,885	25,941
DC9-80	63,503	36,177
DC10-10	206,384	111,086
DC10-40	251,744	122,952
Lockheed L1011-500	231,332	111,357
Fokker F28-4000	33,112	17,546
Rombac-111-560	45,200	24,386
VFW-Fokker 614	19,958	12,179
BAe 146-200	40,596	21,999
A300-B4-200	164,999	88,500
A310-202	131,995	76,616
Ilyushin-Il-62M	162,000	69,400
Tupolev-154	90,000	43,499
Boeing 787-8	227,930	117,707
A380-800	559,993	270,012
A330-200	229,998	120,499
Airbus A320	73,498	42,100
Boeing 777-200	229,518	140,659
A350-1000 Jet-A	316,000	155,129
A350-1000 100% SPK	313,404	155,314

SI 8.2 LH_2 aircraft landing weight analysis

Considering an emergency situation, the landing weight of an aircraft is an important factor. The safe landing weight is dependent on the structural weight of the aircraft. Roskam [94] recommends 0.84 to be an average permissible ratio of the aircraft landing weight and the aircraft's permissible take-off weight, for a transport jet. In the event of an emergency landing immediately after take-off, the pilot performs fuel jettison or dumps the conventional Jet-A

fuel in air so that the aircraft weight goes below its permissible landing weight. However, for an aircraft powered by hydrogen fuel, this highly flammable fuel cannot be dumped into the atmosphere. The present research uses the same MTOW limit (316 tonne) for both Jet-A and LH_2 aircraft. As discussed earlier, for LH_2 fuel there is a net reduction in the aircraft GTOW of 15% from the permissible weight, or $GTOW_{LH2}$ = 0.85 MTOW. During engine start, taxi-out and take-off, LH_2 fuel will consumed and this would further reduce this aircraft weight. The GTOW of this LH_2 aircraft is similar to the average permissible landing weight of the baseline aircraft (structure). This means that there might not be a need to conduct fuel jettison of a highly flammable hydrogen fuel in the event of an emergency landing. This finding is of significance considering the safety issue associated with LH_2 use in a passenger aircraft.

SI 8.3 Off-design point analysis

Figure SI 6 shows the comparison of OEW/GTOW for Jet-A, 100% SPK and LH_2 aircraft at different range and payload (load factor) combinations. It is to be noted that at the off-design points, the OEW for a given fuel case is constant and the GTOW (sum of OEW, payload weight and $W_{F,total}$) varies with flight range/distance to be travelled. For a given payload/load factor case, the $W_{F,total}$ increases (and thus GTOW increases) with increasing range. LH_2 has higher gravimetric energy density than Jet-A (and 100% SPK) and hence relatively less fuel weight is added to the aircraft as compared to Jet-A case. Therefore, the drop in OEW/GTOW is steeper for Jet-A case (and 100% SPK) than LH_2 case with increasing range. This is observed despite the fact that the OEW of the LH_2 aircraft is more than that for the corresponding Jet-A aircraft. For 100% SPK, since the OEW is slightly higher (due to negative volumetric density effects that needs 0.25 m of additional fuselage) and the GTOW is slightly lower (due to positive gravimetric density effects) than Jet-A, OEW/GTOW is slightly higher than Jet-A at all load factor – range combinations.

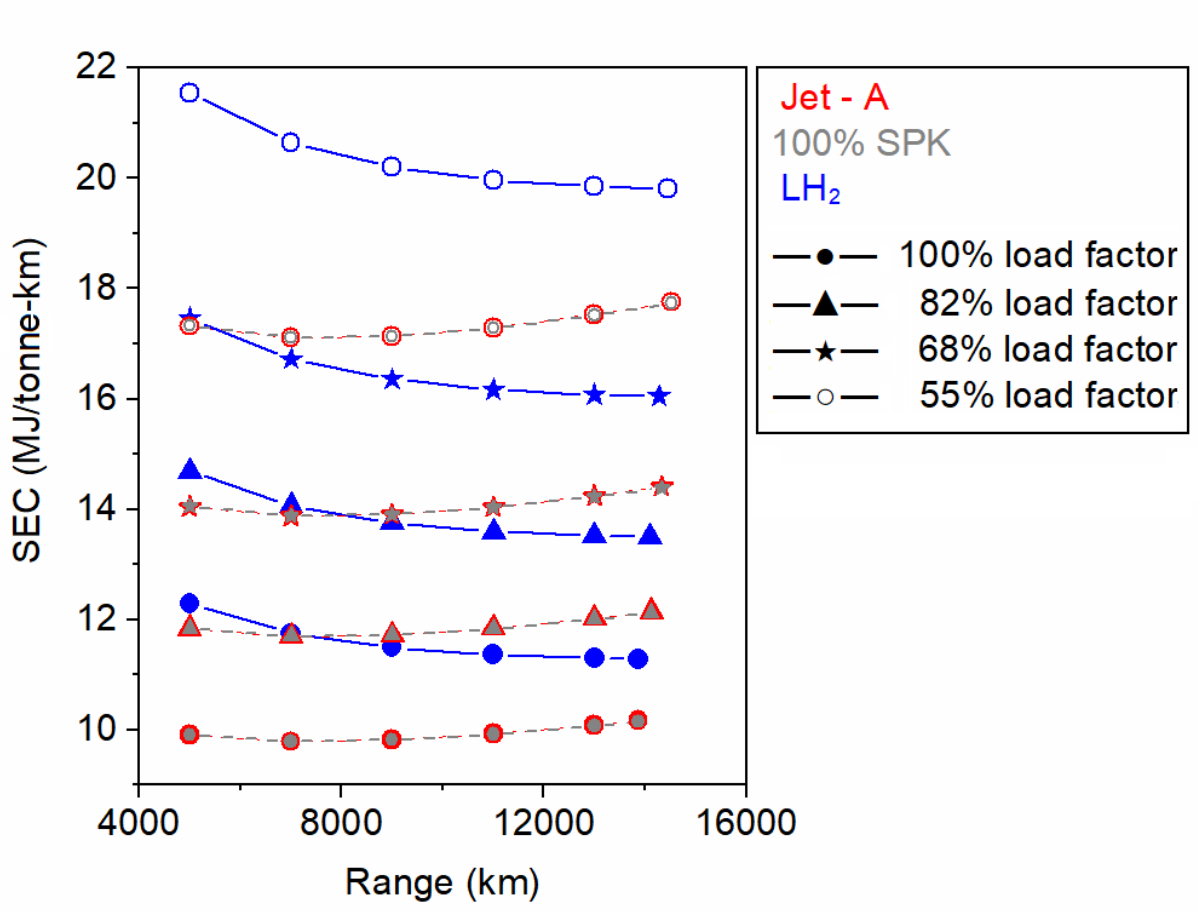

Figure SI 4. SEC comparison for Jet-A, 100% SPK and LH_2 aircraft at different range and payload (load factor) combinations

It was observed from Figure 7 (paper) and Figure SI 4 that for a given passenger – load factor case, LH_2 aircraft consumes more energy than Jet-A aircraft. LH_2 aircraft has a longer fuselage than the corresponding Jet-A aircraft, and therefore a penalty is observed on its aerodynamic performance. Figure SI 7 show the L/D comparison of different fuel cases at different range and load factor combinations. Figure SI 8 and Figure SI 9 show the lift coefficient (C_L) and drag coefficient (C_D) comparison of different fuel cases at different range and load factor combinations. It can be observed that for a given passenger – load factor case the L/D of LH_2 aircraft is lesser than the corresponding Jet-A aircraft. The GTOW of Jet-A aircraft is greater than the corresponding LH_2 aircraft. According to equation SI 3 (paper), the C_L for the Jet-A aircraft is expected to be greater and this is observed in Figure SI 8. Likewise,

increasing the range increases the $W_{F,total}$ and thus the GTOW. Resultantly, C_L (or lift) increases with increasing range and this is observed from Figure SI 8. The C_D calculated here includes the parasitic and lift-induced drag (equation SI 1). For a given LH_2 aircraft case, the OEW is fixed. Therefore, for a given aircraft, with increasing range the parasitic drag remains constant. As discussed above, C_L increases with increasing range and therefore the lift-induced drag also increases. Thus, for a given aircraft case, C_D increases with range. This is observed from Figure SI 9. Overall, both C_L and C_D increase with range for a given aircraft case.

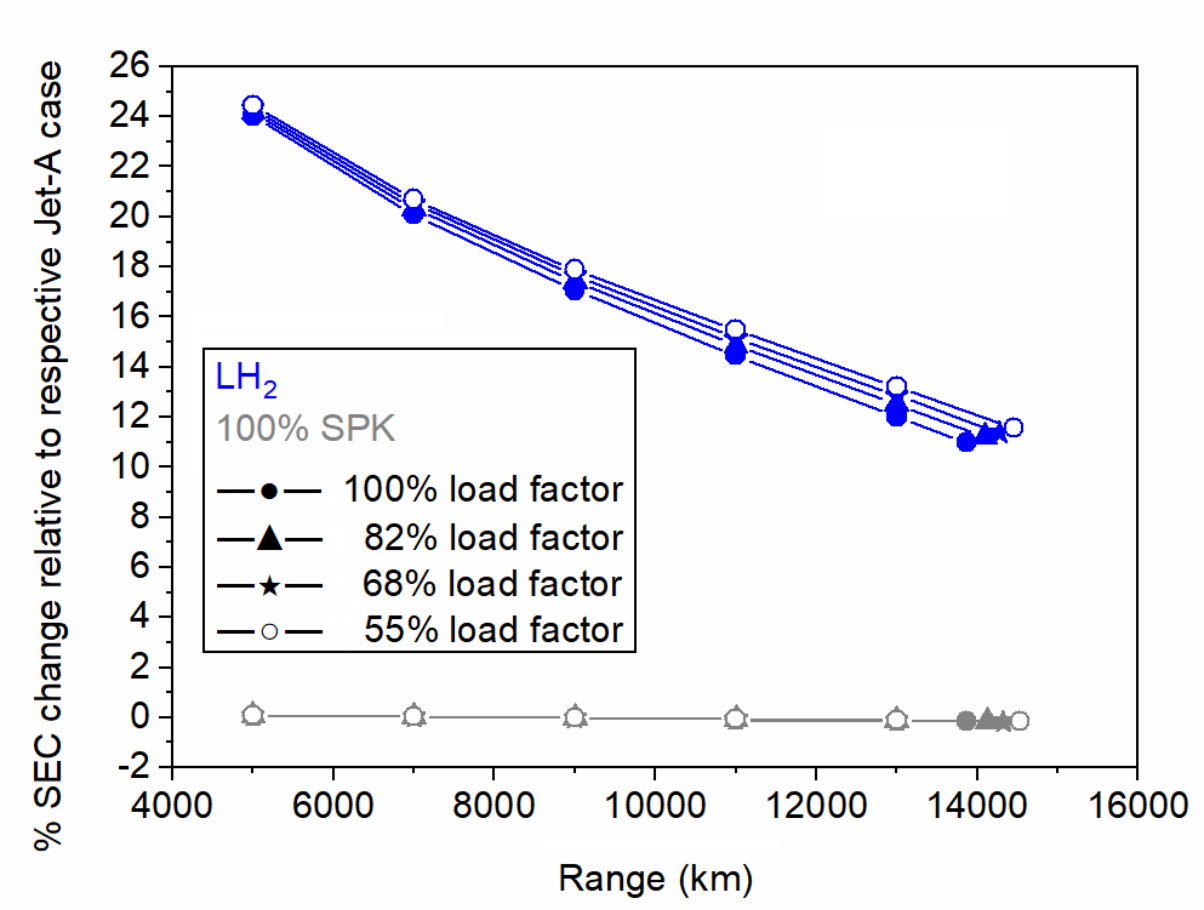

Figure SI 5. Comparison of percent change in SEC for LH_2 and 100% SPK relative to the Jet-A aircraft at different range and payload (load factor) combinations

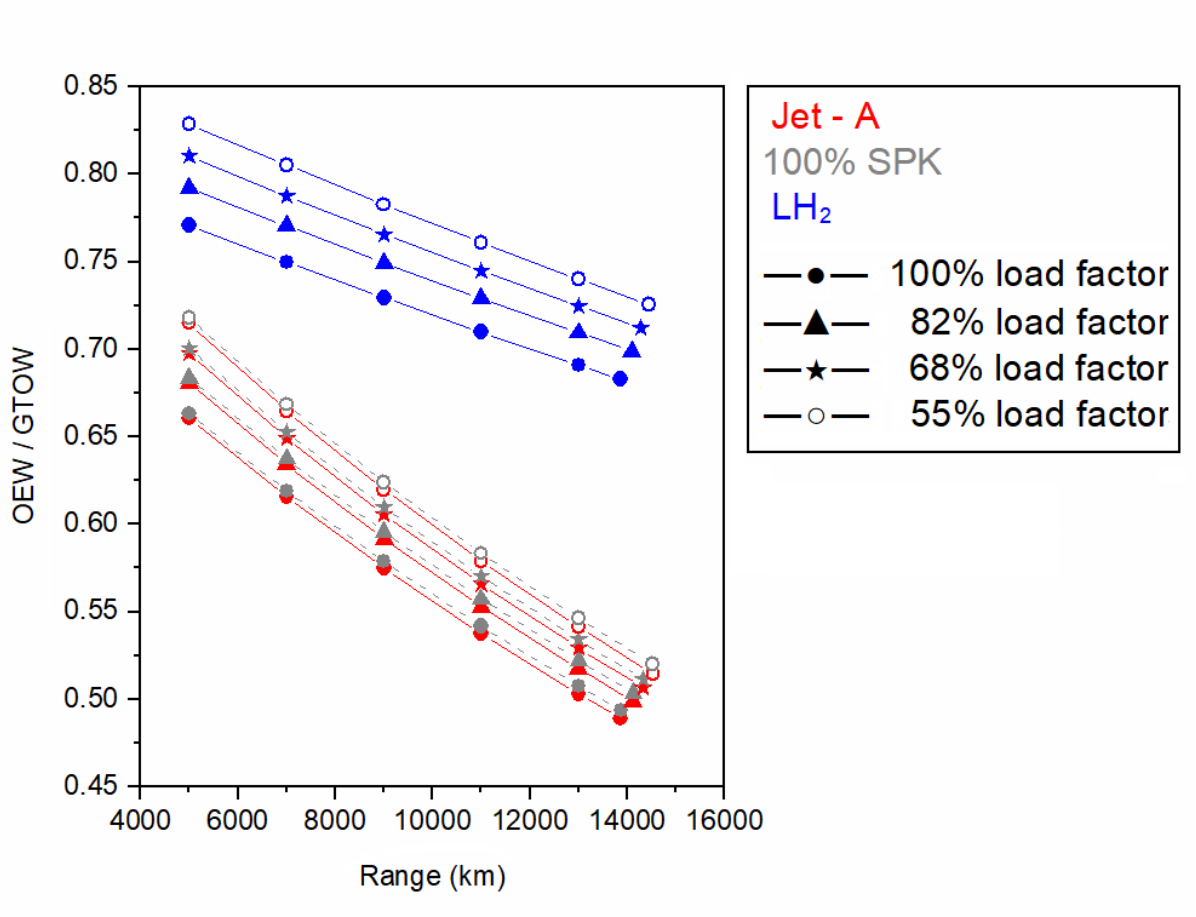

Figure SI 6. Comparison of OEW/GTOW ratio for Jet-A, 100% SPK and LH_2 aircraft at different range and payload (load factor) combinations

For a given aircraft case, the increase in C_L is greater than the increase in C_D which results in a net improvement of *L/D* with increasing range as observed in Figure SI 7. For example: C_L at 13,870 km is 1.21 times C_L at 5,000 km whereas C_D at 13,870 km is 1.12 times C_D at 5,000 km for Jet A 100% load factor; and C_L at 13,870 km is 1.07 times C_L at 5,000 km whereas C_D at 13,870 km is 1.04 times C_D at 5,000 km for LH_2 100% load factor. This results in 1.08 times increase and 1.03 times increase in L/D for Jet A 100% load factor and LH_2 100% load factor, respectively.

For 100% SPK, due to the slightly higher gravimetric energy density the GTOW is lower than Jet-A. Thus, according to equation SI 3 (paper), the C_L for the 100% SPK aircraft is expected to be lower than Jet-A and this is observed in Figure SI 8. Additionally, since the

OEW is slightly higher (due to negative volumetric density effects that needs 0.25 m of additional fuselage), the parasitic drag is higher than Jet-A. However, the GTOW is slightly lower and thus the lift induced drag is smaller than Jet-A. Overall, the C_D for the 100% SPK aircraft is lower than Jet-A and this is observed in Figure SI 9. Considering the effects of both C_L and C_D, the effect of lower GTOW of 100% SPK relative to Jet-A results in lower L/D and this is observed in Figure SI 7.

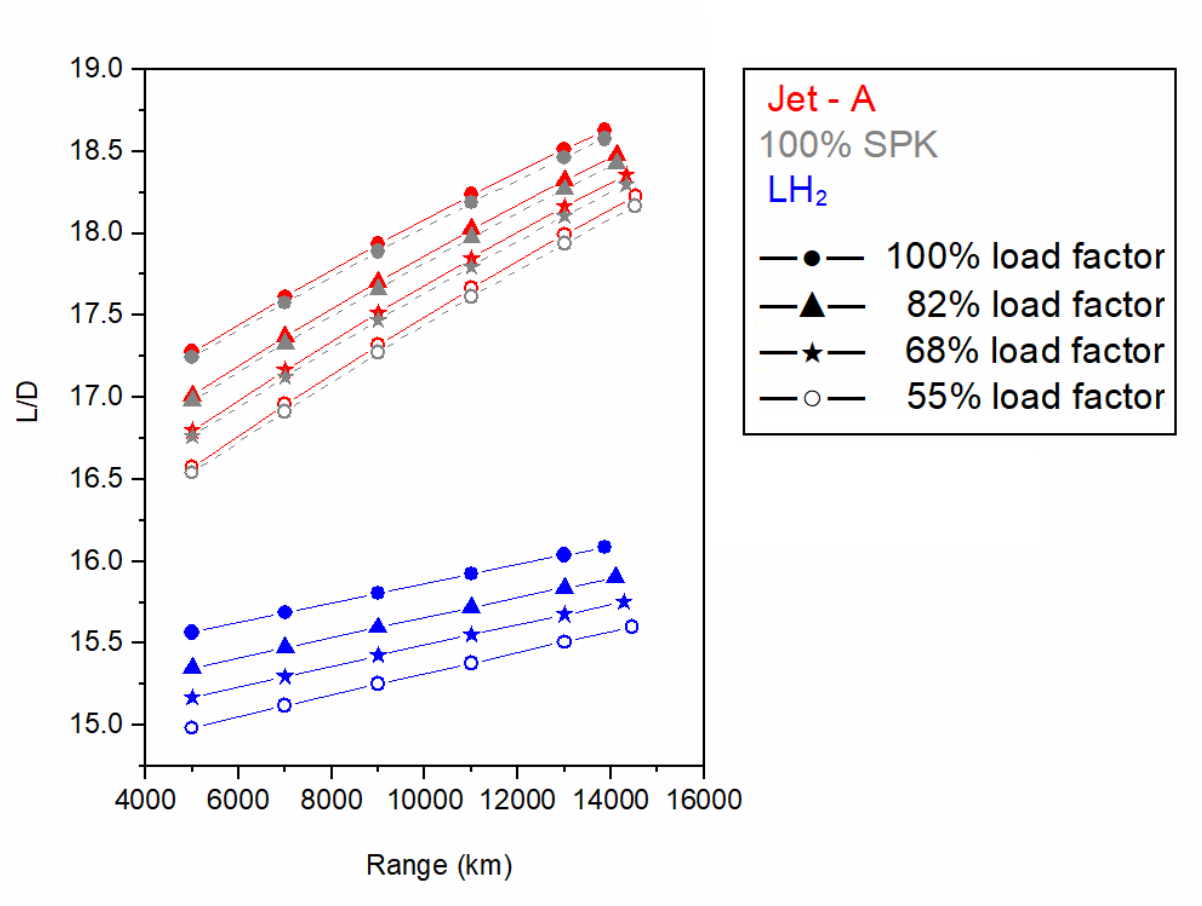

Figure SI 7. Comparison of L/D for Jet-A, 100% SPK and LH_2 aircraft at different range and payload (load factor) combinations

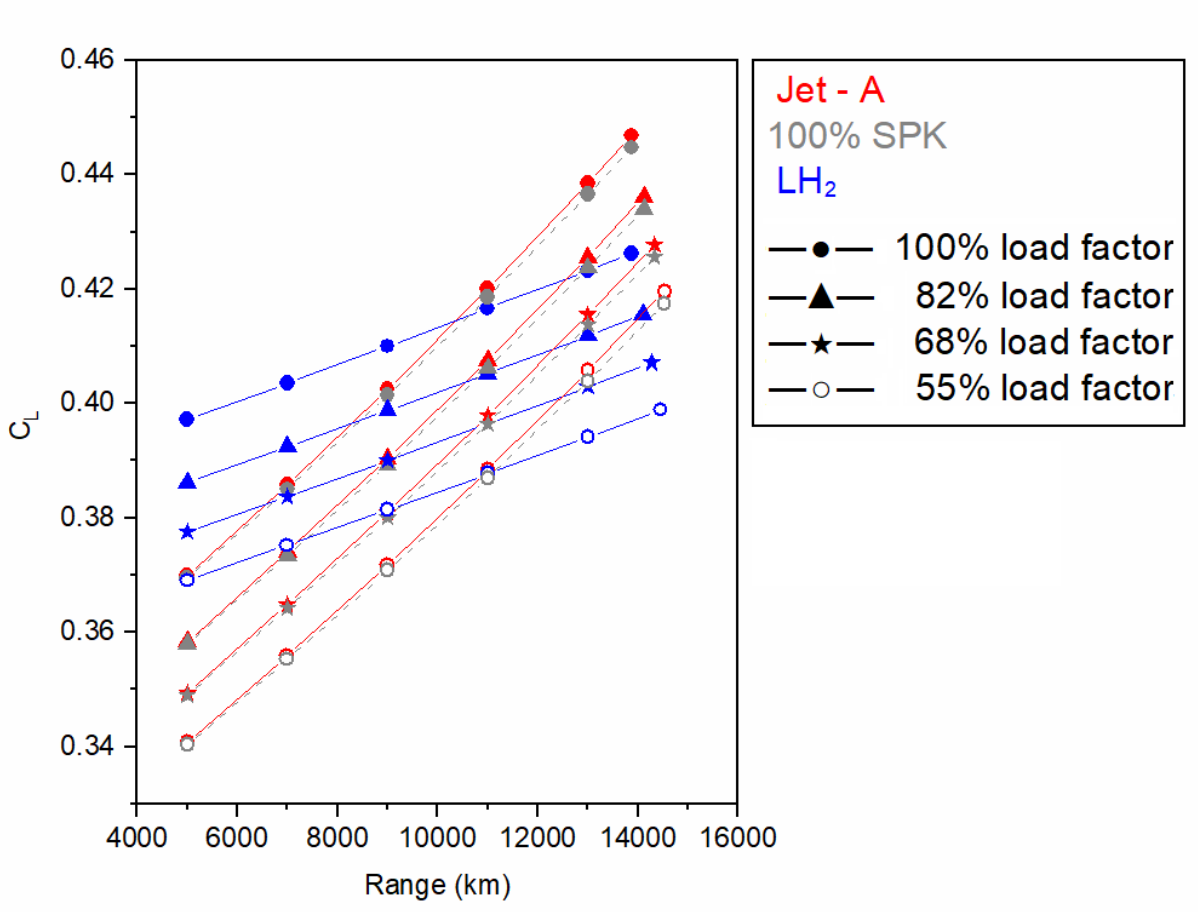

Figure SI 8. Comparison of C_L for Jet-A, 100% SPK and LH_2 aircraft at different range and payload (load factor) combinations

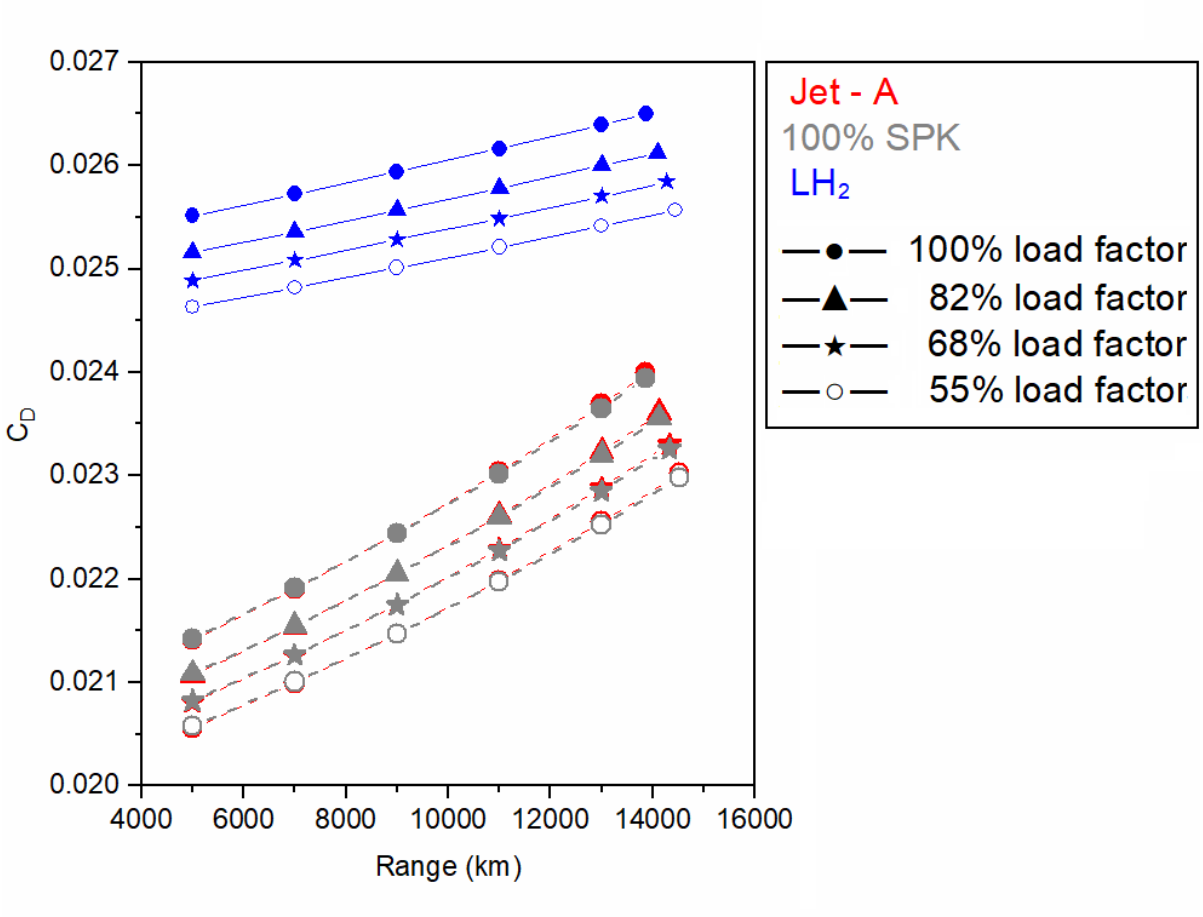

Figure SI 9. Comparison of C_D for Jet-A, 100% SPK and LH_2 aircraft at different range and payload (load factor) combinations

SI 9. Detailed author comments

SI 9.1 Fuselage length

The fuselage fineness ratio (FR = length/diameter) of Boeing 777-200 ER and LR both are 10.27 (= 63.7/6.2), and that of Boeing 777-300 ER is (73.9/6.2 =) 11.92 [129]. The FR of Boeing 787-8, 787-9 and 787-10 are 9.69 (= 55.91/5.77), 10.75 (= 62/5.77) and 11.7 (= 67.48/5.77) respectively [130]. The FR of the baseline A350-1000 Jet-A aircraft is known to be 12.12 from Table SI 4. The FR of the LH_2 aircraft modelled in §4.1 of the paper is (99.12/5.96 =) 16.63 (37.2% increase in fuselage length relative to baseline Jet-A aircraft). One of the interesting aircraft cases is the DC-8 Super 60, which has a slender fuselage and has the

fineness ratio of 14.95 (= 55.75/3.73) [131]. Lastly, the FR of Concorde is 16.7 [132]. The Concorde is an exception because it was a supersonic aircraft and had special aerodynamic requirement as compared to the above sub-sonic aircraft. Slender fuselage (high FR) enables higher cruise Mach number flights as the drag divergence number increases [133].

LH_2 aircraft with longer fuselage could have several issues to be addressed. These aircraft could necessitate design and development for increasing the structural strength for the longer fuselage to prevent longitudinal failures. Particularly, longer fuselage for unchanged diameter (high FR) could imply increase in bending of the fuselage and associated stresses. Additionally, increase in fuselage length is associated with a shift in aircraft's centre of gravity. This could mandate an examination on the criteria for positioning of the landing gear and an evaluation on the required take-off and landing speeds to avoid tail-strikes. From a design viewpoint, a longer aircraft might not be safe from flight dynamics perspective. The empennage and control surfaces have to be redesigned and recalibrated for stability.

Moreover, considering an absolute scale for the fuselage length, longer fuselage could affect take-off rotation, turning radius, operations at the airport, and could necessitate longer field length during take-off and landing. Therefore, significantly longer aircraft might not be readily compatible with present day airport infrastructure. The future airport planning and/or redesigning should take these effects into account if significantly longer (than present) LH_2 aircraft are to enter in service.

SI 9.2 Optimization of aircraft

In SI §4.1, it was assumed that the thrust production for Jet-A and alternative fuels is the same. It is observed in §4.1 of the paper that the LH_2 aircraft GTOW reduces by 15% respectively, and thus its thrust/weight ratio (T/W) will be greater than the baseline aircraft. The optimization of the LH_2 aircraft is necessary considering that its GTOW significantly reduces and this decreases the thrust requirement and energy consumption. According to

studies by Dincer [134] and Nojoumi [25], for a LH_2 powered aircraft the thrust requirement reduces and the engine becomes smaller in size (engine weight savings). Reduction in thrust requirement reduces engine weight and associated fuel weight savings, which further reduces the GTOW. Therefore, for a significantly lighter LH_2 aircraft, optimization is necessary considering that a similar *T/W* of the baseline aircraft is to be maintained for this aircraft.

SI 9.3 Embodied emissions and energy

The fuel cost of 100% SPK and LH_2 is completely dependent on the process through which they are manufactured. The other part of the operational cost is the incentive of using of clean alternative fuel such as hydrogen that emits zero carbon in the aircraft's operational phase. The production pathway of 100% SPK and LH_2 also needs to be less carbon intense.

According to the Clean Sky 2 - Fuel Cells and Hydrogen (FCH) joint project report [100], PtL fuel might be a more cost-effective decarbonization solution with an evolutionary tube-wing long-range aircraft instead of LH_2. PtL is similar to SPK in terms of fuel properties. It is to be noted that PtL fuel production uses hydrogen produced from electrolysis (using power produced from renewable energy). Considering process conversion losses in the PtL fuel production (from hydrogen) and that the future LH_2 powered tube-wing aircraft (implementing advanced aircraft technology) could be more energy efficient than present day tube-wing Jet-A aircraft, the LH_2 aircraft powered by hydrogen produced from renewable electricity could be more sustainable than PtL on a life-cycle basis.

More information:

First author's other research work can be found in [6], [8]–[10], [53], [135]–[157].

References

[1] ATAG, "Aviation and climate change," *Air Transport Action Group*, 2020. https://aviationbenefits.org/media/167159/fact-sheet_2_aviation-and-climate-change.pdf (accessed Oct. 01, 2024).

[2] Y. Bicer and I. Dincer, "Life cycle evaluation of hydrogen and other potential fuels for aircrafts," *Int. J. Hydrogen Energy*, vol. 42, no. 16, pp. 10722–10738, Apr. 2017, doi: 10.1016/j.ijhydene.2016.12.119.

[3] D. L. Daggett, R. C. Hendricks, R. Walther, and E. Corporan, "Alternate Fuels for Use in Commercial Aircraft," Apr. 2008, Accessed: Jan. 11, 2019. [Online]. Available: https://ntrs.nasa.gov/search.jsp?R=20080018472

[4] R. W. Stratton, "Life cycle assessment of greenhouse gas emissions and non-CO_2 combustion effects from alternative jet fuels," 2010, Accessed: Jan. 11, 2019. [Online]. Available: https://dspace.mit.edu/handle/1721.1/59694

[5] K. Lokesh, "Techno-economic environmental risk analysis of advanced biofuels for civil aviation," Cranfield University, 2015. Accessed: Jan. 11, 2019. [Online]. Available: https://dspace.lib.cranfield.ac.uk/handle/1826/9243

[6] S. S. Jagtap, "Sustainability assessment of hydro-processed renewable jet fuel from algae from market-entry year 2020: Use in passenger aircrafts," in *16th AIAA Aviation Technology, Integration, and Operations Conference*, Jun. 2016. doi: 10.2514/6.2016-4367.

[7] IATA, "Sustainable Aviation Fuels Sustainable Aviation Fuels: Fact Sheet 2," *International Air Transport Association*, 2020. https://www.iata.org/contentassets/d13875e9ed784f75bac90f000760e998/saf-

technical-certifications.pdf (accessed Apr. 06, 2020).

[8] S. S. Jagtap, “Assessment of feedstocks for blended alcohol-to-jet fuel manufacturing from standalone and distributed scheme for sustainable aviation,” in *AIAA Propulsion and Energy 2019 Forum*, 2019. doi: 10.2514/6.2019-3887.

[9] S. S. Jagtap, “Comparative assessment of manufacturing setups for blended sugar-to-aviation fuel production from non-food feedstocks for green aviation,” in *AIAA Propulsion and Energy 2019 Forum*, 2019. doi: 10.2514/6.2019-4332.

[10] S. S. Jagtap, “Evaluation of blended Fischer-Tropsch jet fuel feedstocks for minimizing human and environmental health impacts of aviation,” in *AIAA Propulsion and Energy 2019 Forum*, 2019. doi: 10.2514/6.2019-4412.

[11] S. Blakey, L. Rye, and C. W. Wilson, “Aviation gas turbine alternative fuels: A review,” *Proc. Combust. Inst.*, vol. 33, no. 2, pp. 2863–2885, Jan. 2011, doi: 10.1016/J.PROCI.2010.09.011.

[12] J. I. Hileman, P. E. Donohoo, and R. W. Stratton, “Energy Content and Alternative Jet Fuel Viability,” *J. Propuls. Power*, vol. 26, no. 6, pp. 1184–1196, Nov. 2010, doi: 10.2514/1.46232.

[13] ANL, “GREET 2021,” *Argonne National Laboratory*, 2021. https://greet.es.anl.gov/

[14] K. Walker, “Canadian 100% biofuel flight tests show significant emission reductions | Eco-Aviation content from ATWOnline,” *Air Transport World*, 2013. http://atwonline.com/eco-aviation/canadian-100-biofuel-flight-tests-show-significant-emission-reductions (accessed Jan. 16, 2019).

[15] M. Kousoulidou and L. Lonza, “Biofuels in aviation: Fuel demand and CO2 emissions evolution in Europe toward 2030,” *Transp. Res. Part D Transp. Environ.*, vol. 46, pp.

166–181, Jul. 2016, doi: 10.1016/J.TRD.2016.03.018.

[16] ATR, “ATR successfully performs test flights with 100% SAF in one engine - ATR,” *ATR*, Feb. 2022. https://www.atr-aircraft.com/presspost/atr-successfully-performs-test-flights-with-100-saf-in-one-engine/ (accessed Jul. 18, 2022).

[17] Rolls Royce, “Rolls-Royce - Rolls-Royce conducts first tests of 100% sustainable aviation fuel for use in business jets,” *Rolls Royce*, 2021. https://www.rolls-royce.com/media/press-releases/2021/01-02-2021-business-aviation-rr-conducts-first-tests-of-100-precent-sustainable-aviation-fuel.aspx (accessed Jul. 18, 2022).

[18] Airbus, “First A380 powered by 100% Sustainable Aviation Fuel takes to the skies ,” *Airbus*, 2022. https://www.airbus.com/en/newsroom/press-releases/2022-03-first-a380-powered-by-100-sustainable-aviation-fuel-takes-to-the (accessed Jul. 18, 2022).

[19] P. Schmidt, V. Batteiger, A. Roth, W. Weindorf, and T. Raksha, “Power-to-Liquids as Renewable Fuel Option for Aviation: A Review,” *Chemie Ing. Tech.*, vol. 90, no. 1–2, pp. 127–140, Jan. 2018, doi: 10.1002/cite.201700129.

[20] D. Verstraete, P. Hendrick, P. Pilidis, and K. Ramsden, “Hydrogen fuel tanks for subsonic transport aircraft,” *Int. J. Hydrogen Energy*, vol. 35, no. 20, pp. 11085–11098, Oct. 2010, doi: 10.1016/j.ijhydene.2010.06.060.

[21] S. K. Mital, J. Z. Gyekenyesi, S. M. Arnold, R. M. Sullivan, J. M. Manderscheid, and P. L. N. Murthy, “Review of Current State of the Art and Key Design Issues With Potential Solutions for Liquid Hydrogen Cryogenic Storage Tank Structures for Aircraft Applications,” 2006. Accessed: Jan. 01, 2020. [Online]. Available: https://ntrs.nasa.gov/archive/nasa/casi.ntrs.nasa.gov/20060056194.pdf

[22] H. Kobayashi, A. Hayakawa, K. D. K. A. Somarathne, and E. C. Okafor, “Science and

technology of ammonia combustion," *Proc. Combust. Inst.*, vol. 37, no. 1, pp. 109–133, 2019, doi: 10.1016/j.proci.2018.09.029.

[23] J. L. Toof, "A model for the prediction of thermal, prompt, and fuel NOX emissions from combustion turbines," *J. Eng. Gas Turbines Power*, vol. 108, no. 2, pp. 340–347, 1986, doi: 10.1115/1.3239909.

[24] P. Kumar, "An experimental and numerical study of NOx formation mechanisms in NH3-H2-Air flames," Iowa State University, 2012. Accessed: Dec. 28, 2019. [Online]. Available: https://pdfs.semanticscholar.org/88b2/4d4446889dd608775e933f93f7a95859c9f7.pdf

[25] H. Nojoumi, I. Dincer, and G. F. Naterer, "Greenhouse gas emissions assessment of hydrogen and kerosene-fueled aircraft propulsion," *Int. J. Hydrogen Energy*, vol. 34, no. 3, pp. 1363–1369, Feb. 2009, doi: 10.1016/J.IJHYDENE.2008.11.017.

[26] B. Khandelwal, A. Karakurt, P. R. Sekaran, V. Sethi, and R. Singh, "Hydrogen powered aircraft: The future of air transport," *Progress in Aerospace Sciences*, vol. 60. Elsevier Ltd, pp. 45–59, 2013. doi: 10.1016/j.paerosci.2012.12.002.

[27] S. Rondinelli, A. Gardi, R. Kapoor, and R. Sabatini, "Benefits and challenges of liquid hydrogen fuels in commercial aviation," *Int. J. Sustain. Aviat.*, vol. 3, no. 3, p. 200, 2017, doi: 10.1504/ijsa.2017.086845.

[28] M. Prewitz, A. Bardenhagen, and R. Beck, "Hydrogen as the fuel of the future in aircrafts – Challenges and opportunities," *Int. J. Hydrogen Energy*, vol. 45, no. 46, pp. 25378–25385, Sep. 2020, doi: 10.1016/J.IJHYDENE.2020.06.238.

[29] B. Yang, M. Mane, and W. A. Crossley, "An Approach to Evaluate Fleet Level CO2 Impact of Introducing Liquid-Hydrogen Aircraft to a World-Wide Network," Jun.

2022, doi: 10.2514/6.2022-3313.

[30] F. Svensson, “Potential of reducng the environmental impact of civil subsonic aviation by using liquid hydrogen,” Cranfield University, 2005. Accessed: Jun. 17, 2022. [Online]. Available: https://dspace.lib.cranfield.ac.uk/handle/1826/10726

[31] Airbus, “Liquid Hydrogen Fuelled Aircraft-System Analysis: CRYOPLANE Final Technical report,” 2003. https://www.fzt.haw-hamburg.de/pers/Scholz/dglr/hh/text_2004_02_26_Cryoplane.pdf (accessed Dec. 30, 2019).

[32] D. Silberhorn, G. Atanasov, J.-N. Walther, and T. Zill, “ASSESSMENT OF HYDROGEN FUEL TANK INTEGRATION AT AIRCRAFT LEVEL,” *Inst. Transp. Res.*, 2019.

[33] V. Cipolla, D. Zanetti, K. A. Salem, V. Binante, and G. Palaia, “A Parametric Approach for Conceptual Integration and Performance Studies of Liquid Hydrogen Short–Medium Range Aircraft,” *Appl. Sci. 2022, Vol. 12, Page 6857*, vol. 12, no. 14, p. 6857, Jul. 2022, doi: 10.3390/APP12146857.

[34] A. Gomez and H. Smith, “Liquid hydrogen fuel tanks for commercial aviation: Structural sizing and stress analysis,” *Aerosp. Sci. Technol.*, vol. 95, p. 105438, Dec. 2019, doi: 10.1016/j.ast.2019.105438.

[35] F. Troeltsch, M. Engelmann, F. Peter, J. Kaiser, M. Hornung, and A. E. Scholz, “Hydrogen powered long haul aircraft with minimized climate impact,” *AIAA Aviat. 2020 FORUM*, p. 14, 2020, doi: 10.2514/6.2020-2660.

[36] P.-J. Proesmans and R. Vos, “Comparison of Future Aviation Fuels to Minimize the Climate Impact of Commercial Aircraft,” Jun. 2022, doi: 10.2514/6.2022-3288.

[37] V. Grewe *et al.*, “Assessing the climate impact of the AHEAD multi-fuel blended wing body,” *Meteorol. Zeitschrift*, vol. 26, no. 6, pp. 711–725, 2017, doi: 10.1127/METZ/2016/0758.

[38] A. Newby, “Toward Sustainable Aviation,” *Keynote at AIAA Propulsion and Energy Forum 2019*. American Institute of Aeronautics and Astronautics, 2019. Accessed: Jan. 02, 2020. [Online]. Available: https://livestream.com/AIAAvideo/PropEnergy2019/videos/195347621

[39] German-Environment-Agency, “Power-to-Liquids Potentials and Perspectives for the Future Supply of Renewable Aviation Fuel,” *German Environment Agency*, 2016. https://www.umweltbundesamt.de/sites/default/files/medien/377/publikationen/161005_uba_hintergrund_ptl_barrierrefrei.pdf (accessed Mar. 10, 2019).

[40] World Economic Forum, “Target True Zero Unlocking Sustainable Battery and Hydrogen-Powered Flight - Insight Report,” 2022. Accessed: Aug. 05, 2022. [Online]. Available: https://www3.weforum.org/docs/WEF_Target_True_Zero_Aviation_ROUND_2022.pdf

[41] D. Carrington, “Solar plane makes history after completing round-the-world trip | Environment | The Guardian,” *The Guardian*, Jul. 26, 2016. Accessed: Jan. 14, 2019. [Online]. Available: https://www.theguardian.com/environment/2016/jul/26/solar-impulse-plane-makes-history-completing-round-the-world-trip

[42] A. Hern, “First ever plane with no moving parts takes flight | Science | The Guardian,” *The Guardian*, Nov. 21, 2018. Accessed: Jan. 14, 2019. [Online]. Available: https://www.theguardian.com/science/2018/nov/21/first-ever-plane-with-no-moving-parts-takes-flight

[43] H. Xu *et al.*, “Flight of an aeroplane with solid-state propulsion,” *Nat. 2018 5637732*, vol. 563, no. 7732, pp. 532–535, Nov. 2018, doi: 10.1038/s41586-018-0707-9.

[44] T. Grönstedt *et al.*, “Ultra Low Emission Technology Innovations for Mid-Century Aircraft Turbine Engines,” in *Volume 3: Coal, Biomass and Alternative Fuels; Cycle Innovations; Electric Power; Industrial and Cogeneration; Organic Rankine Cycle Power Systems*, Jun. 2016, p. V003T06A001. doi: 10.1115/GT2016-56123.

[45] B. J. Brelje and J. R. R. A. Martins, “Electric, hybrid, and turboelectric fixed-wing aircraft: A review of concepts, models, and design approaches,” *Prog. Aerosp. Sci.*, vol. 104, pp. 1–19, Jan. 2019, doi: 10.1016/J.PAEROSCI.2018.06.004.

[46] University-of-Washington, “Lithium-Ion Battery,” *University of Washington*, 2020. https://www.cei.washington.edu/education/science-of-solar/battery-technology/ (accessed May 20, 2021).

[47] Droneii, “Pushing the Boundaries-Drone Energy Sources,” *Drone Industry Insights*, 2017. https://www.droneii.com/wp-content/uploads/2017/06/Drone-Energy-Sources.pdf (accessed Aug. 19, 2020).

[48] C. Pornet and A. T. Isikveren, “Conceptual design of hybrid-electric transport aircraft,” *Prog. Aerosp. Sci.*, vol. 79, pp. 114–135, Nov. 2015, doi: 10.1016/J.PAEROSCI.2015.09.002.

[49] M. Voskuijl, J. van Bogaert, and A. G. Rao, “Analysis and design of hybrid electric regional turboprop aircraft,” *CEAS Aeronaut. J.*, vol. 9, no. 1, pp. 15–25, Mar. 2018, doi: 10.1007/s13272-017-0272-1.

[50] C. Friedrich and P. A. Robertson, “Hybrid-Electric Propulsion for Aircraft,” *J. Aircr.*, vol. 52, no. 1, pp. 176–189, Jan. 2015, doi: 10.2514/1.C032660.

[51] A. W. Schäfer *et al.*, “Technological, economic and environmental prospects of all-electric aircraft,” *Nat. Energy*, vol. 4, no. 2, pp. 160–166, Feb. 2019, doi: 10.1038/s41560-018-0294-x.

[52] S. W. Ashcraft, A. S. Padron, K. A. Pascioni, G. W. Stout, and D. L. Huff, “Review of propulsion technologies for N+3 subsonic vehicle concepts (Report # 20110022435),” 2011. https://ntrs.nasa.gov/citations/20110022435

[53] S. S. Jagtap, “Systems evaluation of subsonic hybrid-electric propulsion concepts for NASA N+3 goals and conceptual aircraft sizing,” *Int. J. Automot. Mech. Eng.*, vol. 16, no. 4, pp. 7259–7286, 2019, doi: https://doi.org/10.15282/ijame.16.4.2019.07.0541.

[54] H. Kim and M.-S. Liou, “Flow simulation and optimal shape design of N3-X hybrid wing body configuration using a body force method,” *Aerosp. Sci. Technol.*, vol. 71, pp. 661–674, Dec. 2017, doi: 10.1016/J.AST.2017.09.046.

[55] J. L. Felder, G. V. Brown, H. DaeKim, and J. Chu, “Turboelectric Distributed Propulsion in a Hybrid Wing Body Aircraft,” 2011. Accessed: Aug. 19, 2020. [Online]. Available: https://ntrs.nasa.gov/citations/20120000856

[56] U. of Cambridge, “Watts up - aeroplanes go hybrid-electric,” *University of Cambridge*, 2014. https://www.cam.ac.uk/research/news/watts-up-aeroplanes-go-hybrid-electric (accessed Jan. 14, 2019).

[57] DLR, “Conceptual study for environment-friendly flight,” *DLR*, 2020. https://www.dlr.de/en/latest/news/2020/02/20200504_conceptual-study-for-environment-friendly-flight (accessed May 26, 2021).

[58] Rolls-Royce, “Rolls-Royce - Rolls-Royce’s all-electric ‘Spirit of Innovation’ takes to the skies for the first time,” *Rolls Royce*, 2021. https://www.rolls-

royce.com/media/press-releases/2021/15-09-2021-rr-all-electric-spirit-of-innovation-takes-to-the-skies-for-the-first-time.aspx (accessed Mar. 20, 2022).

[59] J. Mukhopadhaya and D. Rutherford, “Performance analysis of evolutionary hydrogen-powered aircraft,” *International Council on Clean Transportation*, 2022. https://theicct.org/publication/aviation-global-evo-hydrogen-aircraft-jan22/ (accessed Jun. 04, 2022).

[60] S. Job, M. Campbell, B. Hall, Z. Hamadache, and N. Kumar, “SUSTAINABILITY REPORT - The Lifecycle Impact of Hydrogen-Powered Aircraft,” 2022. Accessed: Jun. 05, 2022. [Online]. Available: https://www.ati.org.uk/wp-content/uploads/2022/03/FZO-STY-REP-0005-FlyZero-Sustainability-Report.pdf

[61] T. Dietl *et al.*, “POLARIS-DESIGN OF A LIQUID HYDROGEN TURBO-ELECTRIC TRANSPORT AIRCRAFT,” 2018. doi: 10.25967/480344.

[62] T. Y. J. Druot, N. Peteilh, P. Roches, and N. Monrolin, “Hydrogen Powered Airplanes, an exploration of possible architectures leveraging boundary layer ingestion and hybridization,” *AIAA Sci. Technol. Forum Expo. AIAA SciTech Forum 2022*, 2022, doi: 10.2514/6.2022-1025.

[63] M. Thoennes, A. Busse, and L. Eckstein, “Forecast of Performance Parameters of Automotive Fuel Cell Systems - Delphi Study Results,” *Fuel Cells*, vol. 14, no. 6, pp. 781–791, Dec. 2014, doi: 10.1002/fuce.201400035.

[64] M. Delgado Gosálvez *et al.*, “Green Flying: Final Report,” *TU Delft*, 2018. https://www.researchgate.net/publication/326294480_The_Greenliner_Green_Flying_Final_Report_DSE_Group_8 (accessed Jan. 02, 2020).

[65] HyPoint, “HyPoint,” 2020. https://hypoint.us/#rec177636847 (accessed Aug. 16,

2020).

[66] B. Garrett-Glaser, “Will Hydrogen Fuel Cells Play a Role in the VTOL Revolution?,” *Aviation Today*, 2020. https://www.aviationtoday.com/2020/04/16/will-hydrogen-fuel-cells-play-a-role-in-the-vtol-revolution/ (accessed Aug. 16, 2020).

[67] PowerCell, “PowerCell S3,” *PowerCell*, 2020. https://bumhan.com/wp-content/uploads/sites/126/2021/02/PowerCell-S3.pdf (accessed Aug. 16, 2020).

[68] EASA, “ICAO Aircraft Engine Emissions Databank,” *EASA*, 2021. https://www.easa.europa.eu/domains/environment/icao-aircraft-engine-emissions-databank (accessed Aug. 16, 2020).

[69] National-Academies-of-Sciences-Engineering-and-Medicine, *Commercial aircraft propulsion and energy systems research: Reducing global carbon emissions*. National Academies Press, 2016. doi: 10.17226/23490.

[70] EASA, “TYPE-CERTIFICATE DATA SHEET for GE90 Series Engines,” *EASA*, 2019. https://www.easa.europa.eu/downloads/7799/en (accessed Aug. 16, 2020).

[71] A. F. B. Abu Kasim, M. S. C. Chan, and E. J. Marek, “Performance and failure analysis of a retrofitted Cessna aircraft with a Fuel Cell Power System fuelled with liquid hydrogen,” *J. Power Sources*, vol. 521, p. 230987, Feb. 2022, doi: 10.1016/J.JPOWSOUR.2022.230987.

[72] S. Nicolay, S. Karpuk, Y. Liu, and A. Elham, “Conceptual design and optimization of a general aviation aircraft with fuel cells and hydrogen,” *Int. J. Hydrogen Energy*, vol. 46, no. 64, pp. 32676–32694, Sep. 2021, doi: 10.1016/J.IJHYDENE.2021.07.127.

[73] E. G. Waddington, J. M. Merret, and P. J. Ansell, “Impact of LH2 Fuel Cell-Electric Propulsion on Aircraft Configuration and Integration,” *AIAA Aviat. Aeronaut. Forum*

Expo. AIAA Aviat. Forum 2021, 2021, doi: 10.2514/6.2021-2409.

[74] G. Vonhoff, "Conceptual Design of Hydrogen Fuel Cell Aircraft: Flying on hydrogen for a more sustainable future," Delft University of Technology, 2021. Accessed: Aug. 05, 2022. [Online]. Available: https://repository.tudelft.nl/islandora/object/uuid%3A8bd63dec-b67b-496b-92bc-3d5c07ff859f

[75] B. J. Brelje and J. R. R. A. Martins, "Aerostructural wing optimization for a hydrogen fuel cell aircraft," *AIAA Scitech 2021 Forum*, pp. 1–18, 2021, doi: 10.2514/6.2021-1132.

[76] F. Nicolosi, V. Marciello, and F. Orefice, "Conceptual Design of a Hydrogen-Propelled Aircraft with Distributed Electric Propulsion," Jun. 2022, doi: 10.2514/6.2022-3205.

[77] C. L. Pastra, G. Cinar, and D. N. Mavris, "Feasibility and benefit assessments of hybrid hydrogen fuel cell and battery configurations on a regional turboprop aircraft," Jun. 2022, doi: 10.2514/6.2022-3290.

[78] J. Kurzke, "GasTurb 13," *GasTurb GmbH*, 2017. https://gasturb.de/software/gasturb.html

[79] J. Kurzke and I. Halliwell, *Propulsion and Power: An Exploration of Gas Turbine Performance Modeling*. Springer International Publishing, 2018. doi: 10.1007/978-3-319-75979-1.

[80] J. Kurzke, "GasTurb 13 Design and Off-Design Performance of Gas Turbines," 2018.

[81] P. P. Walsh and P. Fletcher, *Gas Turbine Performance*. Wiley, 2004. doi: 10.1002/9780470774533.

[82] J. D. Mattingly, W. H. Heiser, and D. T. Pratt, *Aircraft Engine Design, Third Edition*. American Institute of Aeronautics and Astronautics, 2018. doi: https://doi.org/10.2514/4.105173.

[83] N. A. Cumpsty, *Jet propulsion : a simple guide to the aerodynamics and thermodynamic design and performance of jet engines*. 2015.

[84] H. I. H. Saravanamuttoo, G. F. C. Rogers, H. Cohen, P. V. Straznicky, and A. C. Nix, *Gas Turbine Theory*, Seventh. Pearson, 2017. Accessed: Dec. 17, 2019. [Online]. Available: https://www.pearson.com/us/higher-education/program/Cohen-Gas-Turbine-Theory-7th-Edition/PGM1943364.html

[85] A. Goldmann *et al.*, "A Study on Electrofuels in Aviation," *Energies*, vol. 11, no. 2, p. 392, Feb. 2018, doi: 10.3390/en11020392.

[86] D. Verstraete, "The Potential of Liquid Hydrogen for long range aircraft propulsion," Cranfield University, 2009. Accessed: Aug. 27, 2020. [Online]. Available: http://dspace.lib.cranfield.ac.uk/handle/1826/4089

[87] I. A. Waitz., "Lecture: Breguet's range equation," *Lecture notes*, 2008. https://web.mit.edu/16.unified/www/FALL/Unified_Concepts/Breguet-Range-U2-notes-Fall08(2).pdf (accessed Aug. 27, 2020).

[88] G. Kenway *et al.*, "Reducing Aviation's Environmental Impact Through Large Aircraft for Short Ranges," in *48th AIAA Aerospace Sciences Meeting Including the New Horizons Forum and Aerospace Exposition*, Jan. 2010. doi: 10.2514/6.2010-1015.

[89] RAeS, "Air Travel - Greener by Design The Technology Challenge, Report of the Technology Sub-Group," 2003. Accessed: Mar. 10, 2019. [Online]. Available: https://www.aerosociety.com/Assets/Docs/About_Us/Greener By Design/GbD - 2003

The Tech Challenge.pdf

[90] K. Seeckt, “Aircraft Preliminary Sizing with PreSTo Re-Design of the Boeing B777-200LR Aircraft Preliminary Sizing with PreSTo,” 2008.

[91] G. Dimitriadis, “Introduction to Aircraft Design: Aircraft Performance,” *Université de Liège*, 2017. http://www.ltas-cm3.ulg.ac.be/AERO0023-1/ConceptionAeroPerformances.pdf (accessed Feb. 13, 2020).

[92] J. Henn *et al.*, “Environautics: AIAA Foundation Undergraduate Team Aircraft Design Competition 2009-10,” 2010.

[93] PIANO-X, “Boeing 787 Dreamliner : Analysis,” *PIANO-X*, 2005. https://www.lissys.uk/samp1/index.html (accessed Aug. 28, 2020).

[94] J. Roskam, *Airplane Design. Part I: Preliminary Sizing of Airplanes*. DAR Corporation, 2005.

[95] C. L. Nickol and L. A. McCullers, “Hybrid Wing body configuration system studies,” in *47th AIAA Aerospace Sciences Meeting including the New Horizons Forum and Aerospace Exposition*, 2009. doi: 10.2514/6.2009-931.

[96] D. Scholz, “Drag Prediction,” *Lecture notes*, 2017. https://www.fzt.haw-hamburg.de/pers/Scholz/HOOU/AircraftDesign_13_Drag.pdf (accessed Aug. 28, 2020).

[97] D. Raymer, *Aircraft Design: A Conceptual Approach, Sixth Edition*. Washington, DC: American Institute of Aeronautics and Astronautics, Inc., 2018. doi: 10.2514/4.104909.

[98] P. L. Varghese, “Weight and CG estimation,” *Lecture notes University of Texas, Austin*, 1999. https://www.ae.utexas.edu/~plv955/class/aircraft/weights2.PDF

(accessed Aug. 28, 2020).

[99] Z. Goraj, “Design and Optimisation of Fuel Tanks for BWB Configurations,” *Arch. Mech. Eng.*, vol. 63, no. 4, pp. 605–617, Dec. 2016, doi: 10.1515/meceng-2016-0034.

[100] CleanSky2-FCH, “Hydrogen-powered aviation,” *CleanSky2 - Fuel Cell Hydrogen*, 2020. https://www.fch.europa.eu/sites/default/files/FCH Docs/20200720_Hydrogen Powered Aviation report_FINAL web.pdf (accessed May 03, 2021).

[101] C. Winnefeld, T. Kadyk, B. Bensmann, U. Krewer, and R. Hanke-Rauschenbach, “Modelling and Designing Cryogenic Hydrogen Tanks for Future Aircraft Applications,” *Energies*, vol. 11, no. 1, p. 105, Jan. 2018, doi: 10.3390/en11010105.

[102] G. Polek, “HyPoint Extends Hydrogen Flight Range with New Ultralight Fuel Tanks,” *FutureFlight*, Mar. 29, 2022. https://www.futureflight.aero/news-article/2022-03-29/hypoint-extends-hydrogen-flight-range-new-ultralight-fuel-tanks (accessed Jul. 22, 2022).

[103] J. Sjöberg, J. Smith, O. Haglund Nilsson, P. Emanuelsson, and S. Otlu, “Liquid Hydrogen Tanks for Low-Emission Aircraft,” Chalmers University of Technology, 2021. Accessed: Aug. 03, 2022. [Online]. Available: https://odr.chalmers.se/handle/20.500.12380/302666

[104] Air-Liquide, “Hydrogen storage on board aeronef and ground infrastructure : Air Liquide Advanced Technologies-Workshop on aeronautical applications of fuel cell and hydrogen technologies,” *FCH - CleanSky joint workshop*, 2015.

[105] Wessington-Cryogenics, “ISO VAC 40 LNG : 40 ft LNG Iso Container,” *Wessington Cryogenics*, 2020. https://wessingtoncryogenics.com/products/liquefied-natural-gas-containers/iso-vac-40-lng/ (accessed Sep. 15, 2021).

[106] I. Dincer and C. Zamfirescu, “Sustainable Hydrogen Production,” *Elsevier*, 2016. https://books.google.co.uk/books/about/Sustainable_Hydrogen_Production.html?id=c7h0BgAAQBAJ&redir_esc=y (accessed Aug. 28, 2020).

[107] Airbus, “A350 AIRCRAFT CHARACTERISTICS AIRPORT AND MAINTENANCE PLANNING,” *Airbus*, 2020. https://www.airbus.com/sites/g/files/jlcbta136/files/2021-11/Airbus-Commercial-Aircraft-AC-A350-900-1000.pdf

[108] M. Burzlaff and I. D. Scholz, “Project Aircraft Fuel Consumption-Estimation and Visualization,” 2017. doi: 10.7910/DVN/2HMEHB.

[109] National-Academies-of-Sciences-Engineering-and-Medicine, *Commercial Aircraft Propulsion and Energy Systems Research*. Washington, D.C.: National Academies Press, 2016. doi: 10.17226/23490.

[110] Airbus, “Airbus A350 XWB,” *Airbus*, 2014. https://web.archive.org/web/20131129074833/http://www.airbus.com/aircraftfamilies/passengeraircraft/a350xwbfamily/technology-and-innovation/ (accessed Nov. 09, 2022).

[111] M. Gerzanics, “FLIGHT TEST: Airbus A350-1000 takes growth in its stride | In depth | Flight Global,” *Flight-Global*, 2018. https://www.flightglobal.com/in-depth/flight-test-airbus-a350-1000-takes-growth-in-its-stride/128532.article (accessed Nov. 09, 2022).

[112] D. S. Gerren, “Design, Analysis, and Control of a Large Transport Aircraft Utilizing Selective Engine Thrust as a Backup System for the Primary Flight Control,” *NASA*, 1995. https://ntrs.nasa.gov/api/citations/19960003535/downloads/19960003535.pdf (accessed Nov. 09, 2022).

[113] Engineering-toolbox, “U.S. Standard Atmosphere,” *Engineering-toolbox*, 2003. https://www.engineeringtoolbox.com/standard-atmosphere-d_604.html (accessed Aug. 27, 2020).

[114] A. K. Kundu, M. A. Price, and D. Riordan, *Conceptual Aircraft Design : an Industrial Perspective.*, First. John Wiley & Sons, Incorporated, 2019.

[115] M. R. Kirby, “A methodology for technology identification, evaluation, and selection in conceptual and preliminary aircraft design,” Georgia Institute of Technology, 2001. Accessed: Dec. 17, 2019. [Online]. Available: https://pdfs.semanticscholar.org/3e8f/f5be8491a4f30f4dbb9edce1ff08cfd5b45a.pdf

[116] T. Mommsen, “Airbus A320/321 Quick Change Market Analysis - A Case Study,” *Master’s Theses - Daytona Beach*, Dec. 1994, Accessed: Feb. 08, 2021. [Online]. Available: https://commons.erau.edu/db-theses/252

[117] R. Babikian, “THE HISTORICAL FUEL EFFICIENCY CHARACTERISTICS OF REGIONAL AIRCRAFT FROM TECHNOLOGICAL, OPERATIONAL, AND COST PERSPECTIVES,” 2001. Accessed: Mar. 15, 2019. [Online]. Available: http://web.mit.edu/aeroastro/sites/waitz/publications/Babikian.Thesis.pdf

[118] Aerospaceweb, “Airbus A320 Short to Medium-Range Jetliner,” *Aerospaceweb*, 2011. http://www.aerospaceweb.org/aircraft/jetliner/a320/ (accessed Feb. 09, 2021).

[119] B. Boling, Y. Liu, and E. Stumpf, “Understanding Fleet Impacts of Formation Flight,” 2015.

[120] Digital-Dutch, “1976 Standard Atmosphere Calculator,” *Digital Dutch*, 1999. https://www.digitaldutch.com/atmoscalc/ (accessed Feb. 09, 2021).

[121] R. Babikian, S. P. Lukachko, and I. A. Waitz, “The Historical Fuel Efficiency

Characteristics of Regional Aircraft from Technological, Operational, and Cost Perspectives," 2001. http://web.mit.edu/aeroastro/sites/waitz/publications/Babikian.pdf (accessed Feb. 08, 2021).

[122] All-the-world's-aircraft, "BOEING 767-300 GENERAL MARKET FREIGHTER," *All the world's aircraft*, 2011. http://janes.migavia.com/usa/boeing/boeing-767-300.html (accessed Feb. 09, 2021).

[123] Boeing, "The Boeing 767-300 Freighter - The newest member of the Boeing Frieghter Family," *Boeing*, 2014. http://www.boeing.com/farnborough2014/pdf/BCA/bck-767_5_13_2014.pdf (accessed Feb. 09, 2021).

[124] P. Lironi, "CF6-80C2 engine history and evolution," 2007.

[125] Butterworth-Heinemann, "Civil Jet Aircraft Design - Aircraft Data File - Boeing Aircraft," *Elsevier*, 2001. https://booksite.elsevier.com/9780340741528/appendices/data-a/table-3/table.htm (accessed Feb. 09, 2021).

[126] D. Verstraete, "On the energy efficiency of hydrogen-fuelled transport aircraft," *Int. J. Hydrogen Energy*, vol. 40, no. 23, pp. 7388–7394, Jun. 2015, doi: 10.1016/j.ijhydene.2015.04.055.

[127] G. D. Brewer, *Hydrogen aircraft technology*. CRC Press, 2017. doi: 10.1201/9780203751480.

[128] P. A. Jackson, *IHS Jane's all the world's aircraft : development & production*. Janes Information Group, 2014.

[129] Modern-airliners, "Boeing 777 Specs, what makes this giant twin work?," *Modern-airliners*, 2017. https://modernairliners.com/boeing-777/boeing-777-specs/ (accessed

Aug. 27, 2020).

[130] The-points-guy, “The 787 Dreamliner — What Are the Differences Between a -8, -9 and -10?,” *The points guy*, 2018. https://thepointsguy.co.uk/news/differences-787-8-and-787-9-and-787-10/ (accessed Jan. 22, 2021).

[131] Modern-Airliners, “Douglas DC8,” *Modern Airliners*, 2017. https://modernairliners.com/douglas-dc8/ (accessed Jan. 22, 2021).

[132] D. Scholz, “Fuselage design,” *Lecture notes*, 2017. https://www.fzt.haw-hamburg.de/pers/Scholz/HOOU/AircraftDesign_6_Fuselage.pdf (accessed Jan. 22, 2021).

[133] S. Hoerner, *Fluid-dynamic Drag: Practical Information on Aerodynamic Drag and Hydrodynamic Resistance*. 1965. Accessed: Jan. 22, 2021. [Online]. Available: https://books.google.co.in/books/about/Fluid_dynamic_Drag.html?id=abU8AAAAIAAJ&redir_esc=y

[134] I. Dincer and C. Acar, “A review on potential use of hydrogen in aviation applications,” *Int. J. Sustain. Aviat.*, vol. 2, no. 1, p. 74, 2016, doi: 10.1504/IJSA.2016.076077.

[135] S. Jagtap, A. Strehlow, M. Reitz, S. Kestler, and G. Cinar, “Model-Based Systems Engineering Approach for a Systematic Design of Aircraft Engine Inlet,” in *AIAA SCITECH 2025 Forum*, 2025. doi: https://doi.org/10.2514/6.2025-1410.

[136] S. S. Jagtap, “Non-food feedstocks comparison for renewable aviation fuel production towards environmentally and socially responsible aviation,” in *2019 AIAA Propulsion & Energy Forum*, 2019.

[137] B. Emerson, S. Jagtap, J. M. Quinlan, M. W. Renfro, B. M. Cetegen, and T. Lieuwen, “Spatio-temporal linear stability analysis of stratified planar wakes: Velocity and density asymmetry effects,” *Phys. Fluids*, vol. 28, no. 4, p. 045101, Apr. 2016, doi: 10.1063/1.4943238.

[138] S. S. Jagtap, P. R. N. Childs, and M. E. J. Stettler, “Conceptual design-optimisation of a subsonic hydrogen-powered long-range blended-wing-body aircraft,” *Int. J. Hydrogen Energy*, vol. 96, pp. 639–651, Dec. 2024, doi: 10.1016/J.IJHYDENE.2024.11.331.

[139] S. S. Jagtap, “A heat recovery system designed for shaft-powered aircraft gas turbine engines,” 2016

[140] B. L. Emerson, S. Jagtap, and T. C. Lieuwen, “Stability Analysis of Reacting Wakes: Flow and Density Asymmetry Effects,” in *53rd AIAA Aerospace Sciences Meeting*, Jan. 2015. doi: 10.2514/6.2015-0429.

[141] S. S. Jagtap, “A heat recovery system for shaft-driven aircraft gas turbine engines,” Oct. 29, 2014

[142] S. S. Jagtap, “Heat recuperation system for the family of shaft powered aircraft gas turbine engines,” US10358976B2, 2019 [Online]. Available: https://patents.google.com/patent/US10358976B2/en

[143] S. S. Jagtap, “Evaluation of technology and energy vector combinations for decarbonising future subsonic long-range aircraft,” Imperial College London.

[144] S. S. Jagtap, M. E. J. Stettler, and P. R. N. Childs, “Data in brief: Performance sensitivity of subsonic liquid hydrogen long-range tube-wing aircraft to technology developments”.

[145] S. S. Jagtap, M. E. J. Stettler, and P. R. N. Childs, “Data in brief: Conceptual design-optimisation of futuristic hydrogen powered ultrahigh bypass ratio geared turbofan engine”.

[146] S. S. Jagtap, M. E. J. Stettler, and P. R. N. Childs, “Data in brief: Conceptual design-optimisation of a subsonic hydrogen-powered long-range blended-wing-body aircraft”.

[147] S. S. Jagtap, “Aero-thermodynamic analysis of space shuttle vehicle at re-entry,” *IEEE Aerosp. Conf. Proc.*, vol. 2015-June, Jun. 2015, doi: 10.1109/AERO.2015.7119253.

[148] S. Jagtap and S. Bhandari, “Solar Refrigeration,” *Sardar Patel Int. Conf.*, 2012, [Online]. Available: https://papers.ssrn.com/sol3/papers.cfm?abstract_id=2103115

[149] S. Jagtap and S. Bhandari, “Solar Refrigeration using Triple Fluid Vapor Absorption Refrigeration and Organic Rankine Cycle,” in *Sardar Patel International Conference SPICON 2012 Mechanical*, 2012.

[150] N. Komerath, S. Jagtap, and N. Hiremath, “Aerothermoelastic Tailoring for Waveriders,” in *US Air Force Summer Faculty Fellowship Program*, 2014.

[151] S. S. Jagtap, “Exploration of sustainable aviation technologies and alternative fuels for future inter-continental passenger aircraft.”

[152] S. S. Jagtap, “Identification of sustainable technology and energy vector combinations for future inter-continental passenger aircraft.”

[153] S. S. Jagtap, P. R. N. Childs, and M. E. J. Stettler, “Energy performance evaluation of alternative energy vectors for subsonic long-range tube-wing aircraft,” *Transp. Res. Part D Transp. Environ.*, vol. 115, p. 103588, Feb. 2023, doi: 10.1016/J.TRD.2022.103588.

[154] S. S. Jagtap, P. R. N. Childs, and M. E. J. Stettler, “Performance sensitivity of subsonic liquid hydrogen long-range tube-wing aircraft to technology developments,” *Int. J. Hydrogen Energy*, vol. 50, pp. 820–833, Jan. 2024, doi: 10.1016/J.IJHYDENE.2023.07.297.

[155] S. S. Jagtap, “An Apparatus for Exchanging Heat with Flow in an Annulus,” *J. Eng. Sci. Technol. Rev.*, vol. 10, no. 1, pp. 173–176, 2017, Accessed: Jan. 11, 2019. [Online]. Available: http://www.jestr.org/downloads/Volume10Issue1/fulltext241012017.pdf

[156] S. S. Jagtap, P. R. N. Childs, and M. E. J. Stettler, “Conceptual design-optimisation of a future hydrogen-powered ultrahigh bypass ratio geared turbofan engine,” *Int. J. Hydrogen Energy*, vol. 95, pp. 317–328, Dec. 2024, doi: 10.1016/J.IJHYDENE.2024.10.329.

[157] S. S. Jagtap, M. E. J. Stettler, and P. R. N. Childs, “Data in brief: Energy performance evaluation of alternative energy vectors for subsonic intercontinental tube-wing aircraft”.